Mineralogical Magazine (2022), **86**, 661–676
doi:10.1180/mgm.2022.10

CAMBRIDGE UNIVERSITY PRESS

Article

Special Issue dedicated to Peter Williams

Nomenclature of wöhlerite-group minerals

Fabrice Dal Bo[1*†], Henrik Friis[1] and Stuart J. Mills[2]

[1] Natural History Museum, University of Oslo, P.O. 1172, Blindern, 0318 Oslo, Norway; and [2] Geosciences, Museums Victoria, GPO Box 666, Melbourne, Victoria 3001, Australia

Abstract

A nomenclature and classification scheme for wöhlerite-group minerals has been established. The general formula of minerals belonging to this group is given by $X_8(Si_2O_7)_2W_4$, where $X = Na^+$, Ca^{2+}, Mn^{2+}, Ti^{4+}, Zr^{4+} and Nb^{5+}; and $W = F^-$ and O^{2-}. In addition, they may incorporate significant amounts of Mg^{2+}, Fe^{2+}, Y^{3+} and REE^{3+}, where REE are the lanthanides. The main structural feature of these minerals is the four-columns-wide octahedral walls, which are interconnected through corner sharing and via the disilicate groups. The wöhlerite-group minerals crystallise in different unit-cell settings and symmetries, depending on the cationic ordering in the octahedral walls and the relative position of the disilicate groups. Different combinations of *X* and *W* constituents should be regarded as separate mineral species. In the case of coupled heterovalent substitutions at different crystallographic sites, it is advised to use the site-total charge approach to determine the correct end-member composition. Due to their structural and chemical features, wöhlerite-group minerals can easily form crystals with several micro domains, showing different crystal structures and chemical compositions. In addition, the crystallisation of polytypes is relatively common, although they should not be regarded as distinct mineral species. To date, ten minerals belonging to the wöhlerite group are considered as valid species: baghdadite, burpalite, cuspidine, hiortdahlite, janhaugite, låvenite, moxuanxueite, niocalite, normandite and wöhlerite. Låvenite and normandite are isostructural and are respectively the Zr and Ti end-members of a solid-solution series. Marianoite is discredited, as it is corresponds to wöhlerite. The ideal formula of hiortdahlite is revised as $Na_2Ca_4(Ca_{0.5}Zr_{0.5})Zr(Si_2O_7)_2OF_3$, with one cationic site characterised by a valency-imposed double site-occupancy. These changes have been approved by the IMA–CNMNC (Proposal 20–D).

Keywords: wöhlerite group, cuspidine, wöhlerite, marianoite, hiortdahlite, nomenclature

(Received 5 February 2021; accepted 19 January 2022; Accepted Manuscript published online: 24 January 2022; Associate Editor: Leone Melluso)

Introduction

The first mention of wöhlerite in the literature was made by Scheerer (1843) who studied the mineralogical paragenesis of the syenite pegmatites occurring on Løvøya island, Brevig area, Langesundsfjord, Norway. The chemical analysis performed by Scheerer (1843) indicated that wöhlerite is a silicate containing mainly Na, Ca, Zr and Nb, as well as minor amounts of Mg, Mn and Fe. At the time of wöhlerite's discovery niobium was not officially approved as a distinct chemical element, and consequently Scheerer (1843) had erroneously reported niobium in wöhlerite as tantalum. Among the wöhlerite-group minerals, cuspidine was the first to have its crystal structure solved (Smirnova *et al.*, 1955) and the wöhlerite group is sometimes mentioned as the cuspidine group in the literature (e.g. Merlino and Perchiazzi, 1988; Chakhmouradian *et al.*, 2008). However, as wöhlerite is the first described species of the group the name should be wöhlerite group in accordance with Mills *et al.* (2009). Merlino and Perchiazzi (1988) demonstrated that the nature of the crystal structure of the wöhlerite-group minerals (WGM) permits the crystallisation in different unit-cell settings and the formation of polytypes. In addition, they identified ten different structure-types that are possible within the fixed cell dimension $a \approx b \approx 10.5$ Å and $c \approx 7.3$ Å. The WGM can form multi-domain crystals, as for instance in 'guarinite' from Monte Somma, Italy (Bellezza *et al.*, 2012).

The new definition of the wöhlerite group has been approved by the Commission on New Minerals, Nomenclature and Classification (CNMNC) of the International Mineralogical Association (IMA) (Proposal 20-D; Miyawaki *et al.*, 2020). The wöhlerite group includes mineral species that have the general formula $X_8(Si_2O_7)_2W_4$ (Table 1), where *X* represents the cationic sites typically occupied by Na^+, Ca^{2+}, Mn^{2+}, Fe^{2+}, Ti^{4+}, Zr^{4+} and Nb^{5+}; and where *W* represents anionic sites with F^-, $(OH)^-$ and O^{2-}, which are not bonded to the silicate tetrahedra. The *X* sites have the same general topology and consequently a specific chemical element will have a different *X* site preference in different WGM species. The general formula proposed for WGM is

***Author for correspondence:** Fabrice Dal Bo, Email: fdalbo@uliege.be
†Present address: University of Liège, Department of Geology, Liège, Belgium.
This paper is part of a thematic set that honours the contributions of Peter Williams
Cite this article: Dal Bo F., Friis H. and Mills S.J. (2022) Nomenclature of wöhlerite-group minerals. *Mineralogical Magazine* **86**, 661–676. https://doi.org/10.1180/mgm.2022.10

Table 1. List of minerals belonging to the wöhlerite group.

Mineral and end-member formula	Type of unit-cell*	Structure type*	S.G. *Z*	Unit-cell parameters *a*, Å	*b*, Å	*c*, Å	α, °	β, °	γ, °	Ref.
Cuspidine	I	1	$P2_1/a$	10.919	10.485	7.485	90	109.55	90	[1]
$Ca_8(Si_2O_7)_2F_4$			2							
Låvenite	I	1	$P2_1/a$	10.83	9.98	7.174	90	108.1	90	[2]
$Na_2Ca_2Mn_2Zr_2(Si_2O_7)_2O_2F_2$			2							
Normandite	I	1	$P2_1/a$	10.798	9.835	7.090	90	108.08	90	[3]
$Na_2Ca_2Mn_2Ti_2(Si_2O_7)_2O_2F_2$			2							
Niocalite	I	1	Pa	10.863	10.431	7.370	90	110.1	90	[4]
$Ca_7Nb(Si_2O_7)_2O_3F$			2							
Janhaugite	I	1	$P2_1/n$	10.668	9.787	13.931	90	107.82	90	[5]
$Na_3Mn_3Ti_2(Si_2O_7)_2(OH)_2OF$			4							
Wöhlerite	II	8	$P2_1$	10.823	10.244	7.290	90	109.00	90	[6]
$Na_2Ca_4ZrNb(Si_2O_7)_2O_3F$			2							
Burpalite	III	6	$P2_1/a$	10.1173	10.4446	7.2555	90	90.039	90	[7]
$Na_4Ca_2Zr_2(Si_2O_7)_2F_4$			2							
Baghdadite	III	6	$P2_1/a$	10.432	10.163	7.356	90	90.96	90	[8]
$Ca_6Zr_2(Si_2O_7)_2O_4$			2							
Hiortdahlite	IV	4	$P\bar{1}$	10.9517	10.9251	7.3550	109.369	109.180	83.873	[9, 10]
$Na_2Ca_4(Ca_{0.5}Zr_{0.5})Zr(Si_2O_7)_2OF_3$			2							
Moxuanxueite	IV	4	$P\bar{1}$	10.9527	10.9289	7.3592	109.414	109.889	83.416	[11]
$NaCa_6Zr(Si_2O_7)_2OF_3$			2							
Discredited species										
Marianoite	II	8	$P2_1$	10.8459	10.2260	7.2727	90	109.332	90	[12]
$Na_2Ca_4ZrNb(Si_2O_7)_2O_3F$			2							

S.G. – space group. *see Merlino and Perchiazzi (1988).
References: [1] Saburi *et al.* (1977); [2] Mellini (1981); [3] Perchiazzi *et al.* (2000); [4] Mellini (1982); [5] Annehed *et al.* (1985); [6] Mellini and Merlino (1979); [7] Merlino *et al.* (1990); [8] Biagioni *et al.* (2010); [9] Merlino and Perchiazzi (1985); [10] this work; [11] Qu *et al.* (2020); [12] Chakhmouradian *et al.* (2008).

similar to that of the rinkite group (seidozerite supergroup) minerals (Sokolova and Cámara, 2017), however rinkite- and wöhlerite-group minerals have different structures. The crystal structure of WGM is characterised by four-columns-wide octahedral walls, which interconnect through corner sharing and via the disilicate groups to create a framework (Fig. 1). The cationic ordering in the walls and the relative position of the disilicate groups lead to different symmetries (monoclinic and triclinic). The crystal structure of the borate minerals warwickite and yuanfuliite show the same type of framework, with isolated triangular BO_3 groups replacing the disilicate groups (Bigi *et al.*, 1991; Appel *et al.*, 1999).

Historical synopsis

Cuspidine

Cuspidine, ideally $Ca_8(Si_2O_7)_2F_4$ ($Z = 2$), was described by Scacchi (1876) from Monte Somma, Somma–Vesuvius complex, Italy. Cuspidine occurs in different geological environments such as skarns (Tilley, 1947; Taner *et al.*, 2013), tuff ejecta (Federico and Peccerillo, 2002), pegmatitoid facies of venanzite (Bellezza *et al.*, 2004*a*), calc-silicate xenoliths (Owens and Kremser, 2010), natrocarbonatite (Mitchell and Belton, 2004) and alkaline rocks (Andreeva *et al.*, 2007).

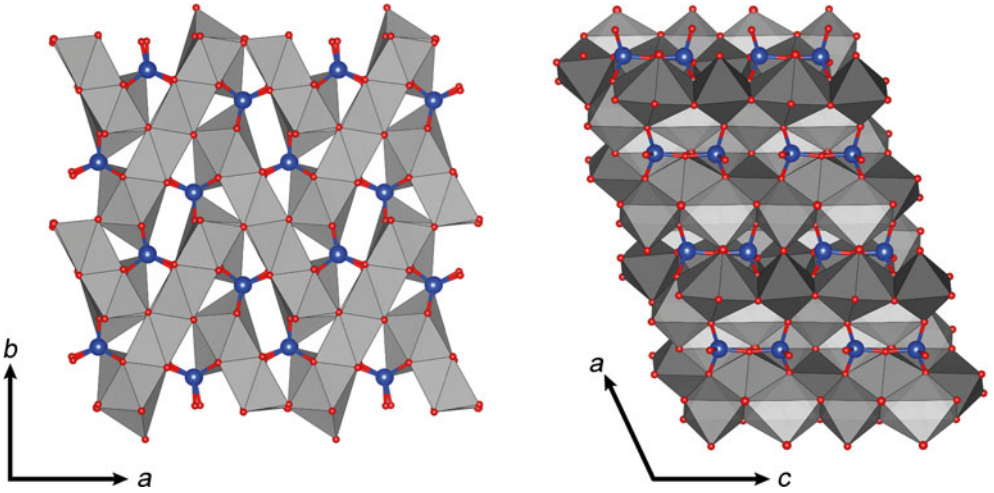

Fig. 1. General view of the structure of the wöhlerite-group minerals. The polyhedra of the octahedral walls are in grey, Si and O atoms are in blue and red, respectively.

https://doi.org/10.1180/mgm.2022.10 Published online by Cambridge University Press

Cuspidine is monoclinic, $P2_1/a$, with $a = 10.906$, $b = 10.521$, $c = 7.518$ Å and $\beta = 109.90°$. The first structural investigation was provided by Smirnova *et al.* (1955) who considered the structure as an array of chains of edge-sharing $Ca(O,F)_6$ octahedra running parallel to the *c* axis, by analogy to the structure of ilvaite, epidote and tilleyite. Subsequent refinement of the cuspidine structure by Saburi *et al.* (1977) concluded that the coordination environments of the Ca sites are not solely octahedral but vary between six-, seven- and eight-fold. There are four Ca sites in total, with an average bond distance of 2.367, 2.404, 2.428 and 2.449 Å. In each column of the wall, the sites alternate between being small or large. Bellezza *et al.* (2004a) reported the incorporation of up to 0.22 Zr atoms per formula unit (apfu) and 0.32 Na apfu in cuspidine, following the substitution mechanism $2Ca^{2+} + F^- \leftrightarrow Na^+ + Zr^{4+} + O^{2-}$. According to their structural model, Zr is incorporated on the small octahedral site lying in the outer columns of the wall (*X*1), whereas Na is incorporated on the large site (*X*3) lying in internal columns and connected by edge-sharing to the Zr-bearing octahedra (Fig. 2). Note that Taner *et al.* (2013) reported cuspidine from the Güneyce–Ikizdere Region in Turkey, with an unusually low F content (1.36 apfu), which may correspond to a hydroxide equivalent. Finally, Krzątała *et al.* (2018) reported from the Hatrurim complex, Israel, a 'uranian cuspidine' containing up to 0.64 U apfu, and only 0.98 F apfu. The oxidation state of uranium remains uncertain, as well as the exact insertion mechanism. Although, considering the similar ionic radii of Ca^{2+} and U^{4+} (U^{5+}) in octahedral coordination, the occurrence of uranium-bearing cuspidine is plausible.

Låvenite and normandite

Låvenite, ideally $Na_2Ca_2Mn_2Zr_2(Si_2O_7)_2O_2F_2$, was described by Brøgger (1884) from nepheline syenite pegmatites occurring on the Låven island, Langesundsfjord area, Norway. Låvenite is now reported from many alkaline localities around the world: Igaliku complex, Greenland (Jones and Larsen, 1985; Friis *et al.*, 2010); Los Archipelago, Guinea (Biagioni *et al.*, 2012); Cerro Boggiani complex, Paraguay (Comin-Chiaramonti *et al.*, 2016); Itatiaia complex, Brazil (Melluso *et al.*, 2017); and Burpala massif, Russia (Vladykin and Sotnikova, 2017).

The crystal structure of låvenite was refined on samples from the Lovozero alkaline massif, Russia (Simonov and Belov, 1960), Langesundsfjord, Norway (Mellini, 1981) and Los Archipelagos, Guinea (Biagioni *et al.*, 2012). Låvenite is monoclinic, $P2_1/a$, with $a = 10.83$, $b = 9.98$, $c = 7.17$ Å and $\beta = 108.1°$. These structural data, as well as the chemical data published elsewhere (see the references listed above) indicate clearly the occurrence of cationic substitution on the four *X* sites (Fig. 2). The larger *X*2 and *X*4 sites are dominated by Ca and Na, respectively. Note that *X*2 usually contains a high amount of Na leading to the mix occupancy close to $Ca_{0.60}Na_{0.40}$. The smallest *X*1 site is dominated by Zr, and the main substitution observed is $Zr^{4+} \leftrightarrow Ti^{4+}$. The last site, *X*3, has an intermediate size (≈ 2.23 Å) and is occupied by a mix of Ca, Fe, Mn and Zr. In låvenite, Mn^{2+} is dominant on *X*3 though the high Ca contents reported in some samples may indicate that Ca could also be dominant, thus leading to a new end-member composition ($Na_2Ca_4Zr_2(Si_2O_7)_2O_2F_2$). The *W*2 site, bonded to the *X*3 and *X*4 sites, is fully occupied by F^-, while the *W*1 site, bonded to the *X*1, *X*3 and *X*4 sites, is populated by O^{2-} which is partially substituted by F^-.

Normandite, ideally $Na_2Ca_2Mn_2Ti_2(Si_2O_7)_2O_2F_2$, is the titanium analogue of låvenite described initially from the Poudrette quarry, Mont Saint-Hilaire, Quebec, Canada (Chao and Gault, 1997). Note that a mineral with similar physical properties and composition had been reported prior to the normandite description from the Khibiny massif and Lovozero massif, Russia (Vlasov, 1966); Tenerife, Canary Islands (Ferguson, 1978) and Tamazeght, Morocco (Khadem Allah, 1993). Perchiazzi *et al.* (2000) refined the crystal structure of normandite from the Poudrette quarry and Amdrup Fjord, Greenland. Normandite is monoclinic, $P2_1/a$, with $a = 10.799$, $b = 9.801$, $c = 7.054$ Å and $\beta = 108.08°$. The normandite structure confirmed the structural model and the cation distribution established in låvenite. Perchiazzi *et al.* (2000) also noted that their samples had an excess of Na and Ca with respect to the expected value of 4 apfu in total, and also had an excess of high-charge cations (Zr and Ti). At the same time, the sum of cations (Mn, Fe and Mg) located on the *X*3 site is significantly below 2 apfu, suggesting that the excess of Ca and Zr is hosted on the *X*3 site with an average bond distance of ≈2.20 Å (Fig. 2).

Baghdadite

Baghdadite, $Ca_6Zr_2(Si_2O_7)_2O_4$, is the only wöhlerite-group mineral without any F^- or OH^- groups. First reported from melilite skarn in contact with diorite, Qala–Dizeh region, Iraq (Hermezi *et al.*, 1986), it has since been described from skarns, calc-silicate marbles and hornfels (Jamtveit *et al.*, 1997; Matsubara and Miyawaki, 1999; Shiraga *et al.*, 2001; Galuskin *et al.*, 2007; Galuskina *et al.*, 2010). The main chemical substitution occurring in baghdadite is the homovalent substitution $Zr^{4+} \leftrightarrow Ti^{4+}$.

Baghdadite is monoclinic, $P2_1/a$, with $a = 10.432$, $b = 10.163$, $c = 7.356$ Å and $\beta = 90.96°$ (Biagioni *et al.*, 2010). In addition to its chemical composition, the crystal structure of baghdadite is also unique for WGM as it shows the edge-sharing of two ZrO_6 octahedra in the internal columns of the wall (Biagioni *et al.*, 2010) (Fig. 2). This structural feature is at odds with the Pauling's fourth rule, which states that high-valence cations tend to not share polyhedron elements (Pauling, 1929). In all other WGM the high-valence cations (Y^{3+}, Ti^{4+}, $Zr^{4+}$and Nb^{5+}) do not share any ligands.

Burpalite

Burpalite, $Na_4Ca_2Zr_2(Si_2O_7)_2F_4$, was found for the first time within a fenitised sandstone in the contact zone of the Burpalinskii alkaline massif, North Transbaikal, Russia (Merlino *et al.*, 1990). It is reported in only a few other localities around the world: Umbozero mine, Lovozero massif, Russia; Vesle Arøya, Langesundsfjorden, Norway; and Nanna pegmatite, Igaliku, Greenland (Friis *et al.*, 2010). Chemical data on burpalite are scarce and the published data on the type material indicates a composition close to the end-member formula.

Burpalite is monoclinic, pseudo-orthorhombic, $P2_1/a$, with $a = 10.117$, $b = 10.445$, $c = 7.255$ Å and $\beta = 90.04°$ (Merlino *et al.*, 1990). Site occupancies indicate that the *X*1 and *X*2 sites are fully occupied by Zr and Ca, respectively. The larger *X*3 and *X*4 sites are mainly populated by Na with minor substitutions of Ca. Bond valence analysis confirms the presence of only F on the *W*2 site, and the replacement of a small amount of F by O on the *W1* site bonded to the Zr polyhedron (Fig. 2).

Structural investigations performed by Merlino *et al.* (1990) also indicate that some crystals of burpalite contain domains with a låvenite-type structure. Burpalite- and låvenite-type

https://doi.org/10.1180/mgm.2022.10 Published online by Cambridge University Press

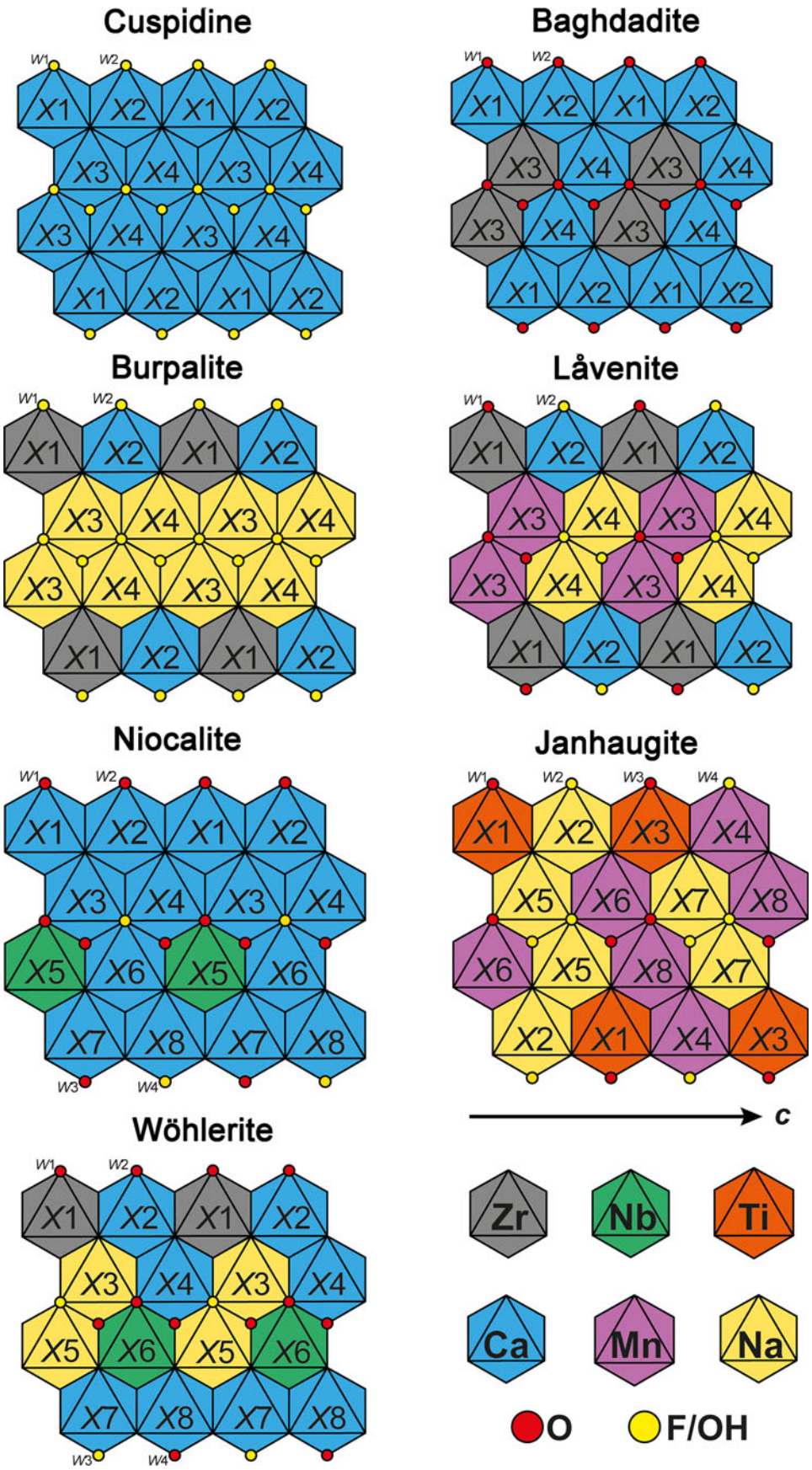

Fig. 2. Schematic and idealised representation of the cationic distribution in the walls of cuspidine, baghdadite, burpalite, låvenite, niocalite, janhaugite and wöhlerite (and marianoite, see text). Normandite has the same cationic distribution as låvenite with *X*1 = Ti.

https://doi.org/10.1180/mgm.2022.10 Published online by Cambridge University Press

structures are related, as they are two distinct ordered members in a family of order–disorder structures. In addition, a so-called 'orthorhombic låvenite' was reported from the Burpalinskii massif (Portnov *et al.*, 1966; Portnov and Sidorenko, 1975). This mineral has the same chemical composition as burpalite, but with a *B*-centred orthorhombic cell, $a = 21.01$, $b = 10.05$ and $c = 7.23$ Å, and is polysynthetically twinned on (100). That unit-cell however, can be transformed to monoclinic, $a = 11.11$, $b = 10.05$, $c = 7.23$ Å and $\beta = 108.99°$, twinned on (100), analogous to the unit-cell of låvenite. Consequently 'orthorhombic låvenite' is a polytype of burpalite (burpalite-1M_2), corresponding to a twinned maximum degree of order (MDO) polytype.

Merlino *et al.* (1990) suggested that isotypic series may occur between burpalite and baghdadite through the substitution $Na^+ + F^- \leftrightarrow Ca^{2+} + O^{2-}$. However, a burpalite–baghdadite series is unlikely because in burpalite the ZrO_6 octahedra are lying in the outer columns of the walls, while in baghdadite they are in the central columns (Fig. 2). Therefore, a transformation of burpalite into baghdadite requires a complete reordering of the cationic octahedral sites.

Niocalite

Niocalite, ideally $Ca_7Nb(Si_2O_7)_2O_3F$, is a rare niobium silicate reported from the Oka complex, Laurentides, Canada (Nickel, 1956), the Badloch quarry, Baden-Württemberg, Germany (Keller and Williams, 1995) and the Ol Doinyo Lengai, Arusha region, Tanzania (Mitchell and Belton, 2004; Reusser, 2010).

Niocalite crystals typically show polysynthetic or contact twinning and therefore the determination of the correct space group was not straightforward. Nickel *et al.* (1958) reports the unit-cell parameters $a = 10.83$, $b = 10.42$, $c = 7.38$ Å and $\beta = 109.40°$, and the probable space group *Pa* or *P*2/*a*. They showed that the twinned crystals have a pseudo-orthorhombic symmetry that is achieved through the twin plane ($\bar{1}02$). Li *et al.* (1966) conducted a structural investigation and proposed a model in $P2_1$, though without taking the twinning into account. The presence of Si_2O_7 groups ambiguously connected to the short edge of the NbO_6 octahedra in the Li *et al.* model prompted Mellini (1982) to reinvestigate the crystal structure of niocalite using the space group *Pa*. Mellini (1982) interpreted the diffraction pattern from twinned niocalite as the result of a twinning on the (100) compositional plane. The same author confirmed the presence of microstructural domains in niocalite through transmission electron microscopy investigations. Although, the structure refinement seems to indicate a disordered distribution of Ca and Nb within two different crystallographic sites (*X*4 and *X*6), it was concluded by Mellini (1982) that Nb and Ca are ordered on their respective sites (Fig. 2). The apparent disorder is the result of the averaging of the intensity data from the two twin-related domains, in which the *X*4 and *X*6 site positions are mutually inverted.

Note that the chemical analysis shows the presence of approximately two F apfu in niocalite, while the end-member formula has only one F apfu. The bond valence analysis shows that only the *W*3 site, which is shared solely by Ca polyhedra, is entirely populated by F. The remaining F content is distributed randomly on the other *W* sites. The incorporation of F on the *W* sites results from the charge balance mechanism linked to the $Ca^{2+} \leftrightarrow Na^+$ substitution, and to the partial replacement of Nb^{5+} by Ti^{4+} and Zr^{4+}.

Wöhlerite

Wöhlerite, ideally $Na_2Ca_4ZrNb(Si_2O_7)_2O_3F$, was reported initially by Scheerer (1843) from the syenite pegmatites occurring on Løvøya island, Brevig area, Langesundsfjord, Norway. Wöhlerite is an abundant mineral throughout the Langesundsfjord (Andersen *et al.*, 2010; Larsen, 2010; Sunde *et al.*, 2018), though also from other syenites and carbonatites around the world (e.g. Mariano and Roeder, 1989; Keller and Williams, 1995; Bellezza *et al.*, 2012; Biagioni *et al.*, 2012; Melluso *et al.*, 2017; Guarino *et al.*, 2019).

Wöhlerite is monoclinic, $P2_1$, with $a = 10.823$, $b = 10.244$, $c = 7.290$ Å and $\beta = 109.00°$ (Mellini and Merlino, 1979). Shibayeva and Belov (1962) and Golyshev *et al.* (1973) performed the first structure refinements on wöhlerite and showed the presence of four-columns-large octahedral walls interconnected by corner sharing and Si_2O_7 diorthosilicate groups. Mellini and Merlino (1979) provided a structure refinement of wöhlerite from Brevig, Norway, confirming the space group and showing that the structure is based on four independent Si sites, four Ca sites, two Na sites, one Zr site and one Nb site (Fig. 2). The bond-valence analysis indicates that only one anionic site is dominated by a monovalent anion. Biagioni *et al.* (2012) have refined the crystal structure of wöhlerite from Los Archipelagos, Guinea, which contains more Mn and F, and less Nb than the Norwegian material.

Chemical data provided by Mariano and Roeder (1989) on wöhlerite from different localities indicate that the chemical composition of wöhlerite is relatively consistent, and they note that the largest variations are observed for the Nb, Ti and F contents. According to the structural model they establish the coupled substitution $Nb^{5+} + O^{2-} \leftrightarrow Ti^{4+} + F^-$. However, the Ti increase is only half of the decrease of the Nb content, thus indicating a replacement of Nb by another chemical element. This is confirmed by subsequent crystal structure refinements in which the Nb site is populated by a significant amount of Mn or Mg (Bellezza *et al.*, 2012; Biagioni *et al.*, 2012). Andersen *et al.* (2010) and Sunde *et al.* (2018) showed only minor chemical variations in wöhlerite from different localities in the Larvik plutonic complex in Norway.

Janhaugite

Described from a sodium-rich alkali feldspar granite (ekerite) at Gjerdingen, Oslo region, Norway (Raade and Mladeck, 1983), janhaugite, ideally $Na_3Mn_3Ti_2(Si_2O_7)_2(OH)_2OF$, is an extremely rare mineral displaying some unique chemical features among the WGM. The Mn content in janhaugite (up to 2.4 apfu) is the highest recorded for any WGM. Electron microprobe analytical (EMPA) data show the presence of roughly one F apfu. Infrared spectroscopy confirmed the presence of OH groups, and the splitting of the O–H stretching frequencies (3550, 3510 and 3460 cm^{-1}) may indicate that OH groups are distributed on three different crystallographic sites (Raade and Mladeck, 1983).

Janhaugite is monoclinic, $P2_1/n$, with $a = 10.668$, $b = 9.787$, $c = 13.931$ Å and $\beta = 107.82°$ (Annehed *et al.*, 1985). The refinement of the crystal structure, coupled with the bond-valence analysis, indicate that only two *W* sites (*W*2 and *W*4) are populated mainly by monovalent anions (Fig. 2). While the sum of (OH + F) should be equal to three to keep the electroneutrality of the mineral, one can assume that the remaining monovalent anions are distributed randomly on the *W*1 and *W*3 sites.

https://doi.org/10.1180/mgm.2022.10 Published online by Cambridge University Press

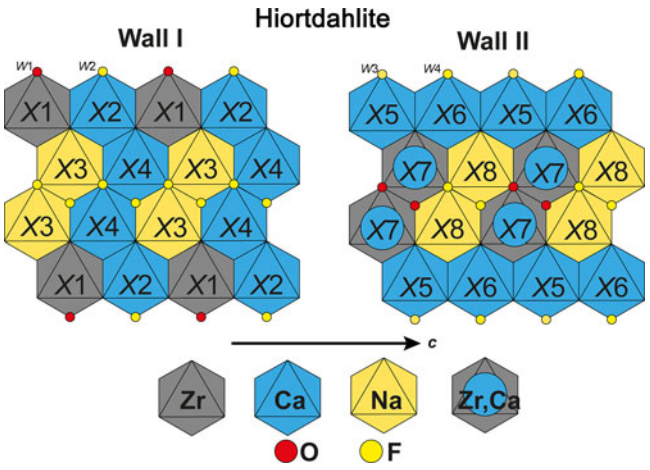

Fig. 3. Schematic and idealised representation of the cationic distribution in the walls of hiortdahlite.

Considering the local environment of the *W*1–*W*4 sites, *W*2 and *W*4 are tri-coordinated, wheras *W*1 and *W*3 are four-coordinated, and it is most likely that the OH groups occupy the *W*2–*W*4 sites. In addition, there are H acceptors in the vicinity of *W*2–*W*4 (≈2.9 Å). Therefore, the end-member formula $Na_3Mn_3Ti_2(Si_2O_7)_2(OH)_2OF$ is proposed for janhaugite, in order to show the ionic distributions on both the *X* and *W* sites, and to follow the rules defined for end-member formula by Hawthorne (2021).

Hiortdahlite

Hiortdahlite, $Na_2Ca_4(Ca_{0.5}Zr_{0.5})Zr(Si_2O_7)_2OF_3$, one of the oldest WGM known, was described from the Langodden pegmatite occurring in the nepheline–syenite of Langesundsfjord, Norway (Brøgger, 1890a, 1890b). Hiortdahlite is observed in several localities across the world and has been studied from the Korgeredaba alkaline Massif, Tuva, Russia (Kapustin and Bykova, 1965); Jingera, Australia (Eggleton *et al.*, 1979) and Los Archipelago, Guinea (Biagioni *et al.*, 2012).

Hiortdahlite is triclinic, $P\bar{1}$, $a = 11.015$, $b = 10.941$, $c = 7.353$ Å, $\alpha = 109.35$, $\beta = 109.88$ and $\gamma = 83.43°$ (Merlino and Perchiazzi, 1985). In addition, in their work on the multi-domains phase called 'guarinite' from Monte Somma, Italy, Bellezza *et al.* (2012) reported one domain isostructural with hiortdahlite (domain IV). In the first structural investigation of hiortdahlite, Merlino and Perchiazzi (1985) identified three crystallographic sites [*M* (*X*7), *NaCa* (*X*8), and *F*3 (*W*2)] where chemical substitutions occur. The *X*8 and *W*2 sites show a mixed occupancy of ($Na_{0.60}Ca_{0.40}$) and ($F_{0.60}O_{0.40}$), respectively (Fig. 3). The cationic substitutions occurring on the *X*7 site are complex, with a broad range of cations that may be incorporated (Fe^{2+}, Mn^{2+}, Ca^{2+} and Zr^{4+}).

In their model, Merlino and Perchiazzi (1985), showed that the average charge of the *X*7 site is +3, and fixed the *X*7 site population to $(Zr_{0.33}Ti_{.16}Ca_{0.16}Mn_{0.16}Fe_{0.16})^{\Sigma 3+}$ according to the chemical data of Brøgger (1890a). Andersen *et al.* (2010) have reanalysed a crystal fragment of the holotype sample (TYHIO sample, NRM no. 530976), and gave the formula $Na_{1.74}Ca_{4.60}Mn_{0.10}Fe_{0.10}Y_{0.03}Ce_{0.01}Zr_{1.16}Nb_{0.11}Ti_{0.09}Hf_{0.02}(Si_2O_7)_2O_{0.6}F_{3.4}$, which is comparable to the chemistry of Brøgger (1890a), $Na_{1.55}Ca_{4.41}Mn_{0.11}Fe_{0.10}REE_{0.03}Ce_{0.01}Zr_{1.32}Ti_{0.14}(Si_2O_7)_2(OH)_{0.5}O_{0.98}F_{2.33}$ (with REE defining lanthanides). New crystallographic and chemical investigations have been performed on samples from the type locality, in order to determine accurately the cationic distribution in the crystal structure. These new data are presented below.

Moxuanxueite

Moxuanxueite, ideally $NaCa_6Zr(Si_2O_7)_2OF_3$, was described recently from the alkaline syenites of the Gejiu intrusion in Honghe Hani and Yi, Autonomous Prefecture, Yunnan Province, China (Qu *et al.*, 2020). The mineral is triclinic, $P\bar{1}$, $a = 10.953$, $b = 10.929$, $c = 7.359$ Å, $\alpha = 109.41$, $\beta = 109.89$ and $\gamma = 83.42°$. Moxuanxueite is isostructural with hiortdahlite, with the *X*7 and *X*8 sites fully occupied by Ca (Table 2).

Chemical compositions of WGM and related species

Chemical classification of WGM

The members of the wöhlerite group show a range of compositions with the main cations being Na, Ca, Fe, Mn, Zr, Ti and

Table 2. Structural formula for the minerals of the wöhlerite group.

One topological wall	$(X1)_2$	$(X2)_2$	$(X3)_2$	$(X4)_2$					$(Si_2O_7)_2$	$(W1)_2$	$(W2)_2$		
Cuspidine	Ca	Ca	Ca	Ca					$(Si_2O_7)_2$	F	F		
Baghdadite	Ca	Ca	Zr	Ca					$(Si_2O_7)_2$	O	O		
Burpalite	Zr	Ca	Na	Na					$(Si_2O_7)_2$	F	F		
Låvenite	Zr	Ca	Mn	Na					$(Si_2O_7)_2$	O	F		
Normandite	Ti	Ca	Mn	Na					$(Si_2O_7)_2$	O	F		
	*X*1	*X*2	*X*3	*X*4	*X*5	*X*6	*X*7	*X*8	$(Si_2O_7)_2$	*W*1	*W*2	*W*3	*W*4
Niocalite	Ca	Ca	Ca	Ca	Nb	Ca	Ca	Ca	$(Si_2O_7)_2$	O	O	O	F
Janhaugite	Ti	Na	Ti	Mn	Na	Mn	Na	Mn	$(Si_2O_7)_2$	$(O_{0.5}F_{0.5})$	OH	$(O_{0.5}F_{0.5})$	OH
Wöhlerite	Zr	Ca	Na	Ca	Na	Nb	Ca	Ca	$(Si_2O_7)_2$	O	O	O	F
Marianoite	Zr	Ca	Na	Ca	Na	Nb	Ca	Ca	$(Si_2O_7)_2$	O	O	O	F
Two topological walls*	*X*1	*X*2	*X*3	*X*4	*X*5	*X*6	*X*7	*X*8	$(Si_2O_7)_2$	*W*1	*W*2	*W*3	*W*4
Hiortdahlite	Zr	Ca	Na	Ca	Ca	Ca	$Ca_{0.5}Zr_{0.5}$	Na	$(Si_2O_7)_2$	O	F	F	F
Moxuanxueite	Zr	Ca	Na	Ca	Ca	Ca	Ca	Ca	$(Si_2O_7)_2$	O	F	F	F

**X*1–*X*4 and *X*5–*X*8 sites are part of the first and second wall, respectively. See references from Table 1 for the other minerals.

https://doi.org/10.1180/mgm.2022.10 Published online by Cambridge University Press

Nb while the main anions are O, F and OH^-. These elements are also the main components of other disilicates with similar optical properties common to alkaline rocks, e.g. rinkite-group minerals of the seidozerite supergroup (Sokolova and Cámara, 2017; Pautov *et al.* 2019). Most petrological studies of alkaline rocks do not utilise techniques other than chemical data to classify minerals. Therefore, we have explored the feasibility of (1) distinguishing wöhlerite-group minerals from related minerals and (2) classifying WGM down to species level solely based on EMPA data. We have used a total of 908 analyses of WGM and related minerals from our own work and the literature: Aarden and Gittins (1974); Ferguson (1978); Eggleton *et al.* (1979); Raade and Mladeck (1983); Hermezi *et al.* (1986); Marino and Roeder (1989); Merlino *et al.* (1990); Keller and Williams (1995); Sharygin *et al.* (1996a,b); Chao and Gault (1997); Jamtveit *et al.* (1997); Stoppa *et al.* (1997); Atencio *et al.* (1999); Perchiazzi *et al.* (2000); Roda-Robles *et al.* (2001); Shiraga *et al.* (2001); Federico and Peccerillo (2002); Christiansen *et al.* (2003); Bellezza *et al.* (2004a, 2004b); Mitchell and Belton (2004); Casillas *et al.* (2008); Chakhmouradian *et al.* (2008); Andersen *et al.* (2010); Friis *et al.* (2010); Owens and Kremser (2010); Bellezza *et al.* (2012); Biagioni *et al.* (2012); Chakrabarty *et al.* (2013); Chen *et al.* (2013); Melluso *et al.* (2014); Rønsbo *et al.* (2014); Comin-Chiaramonti *et al.* (2016); Melluso *et al.* (2017); Chakrabarty *et al.* (2018); Sunde *et al.* (2018) and Guarino *et al.* (2019).

Before attempting a classification or discrimination of species based purely on chemistry, all data were recalculated on the basis of 18 anions. We have maintained the identification of each analytical point as given in the respective papers, i.e. we have not changed mineral identifications. The WGM typically have no substitution on the Si sites and the *X* sites are filled, i.e. there are no, or only limited, vacancies in fresh material. Therefore, only data where $3.9 < \text{Si apfu} < 4.1$ and $7.8 < \Sigma X \text{ apfu} < 8.2$ should be treated. We allow for some variation from ideal stoichiometry due to the challenges of analyses some of these minerals. Of the 908 analytical points 258 did not fulfil these criteria and therefore the following is based on the remaining 650 analyses.

Keller and Williams (1995) used three ternary plots to classify WGMs, and we present our data in two of the same diagrams (Fig. 4). Contrary to the paper by Keller and Williams (1995) our data show significant overlaps between species. For example, hainite-(Y), kochite and rosenbuschite overlap in all plots and partly overlap with låvenite. Conversely, wöhlerite forms a distinct group in Fig. 4a,c,e,f. However, Fig. 4a shows that (i) janhaugite (WGM) overlaps with rinkite-group minerals grenmarite and seidozerite and (ii) låvenite (WGM) overlaps with rosenbuschite (rinkite group, seidozerite supergroup). Figure 4b,e show (i) a strong overlap between four minerals: wöhlerite-group minerals wöhlerite and hiortdahlite and rinkite-group minerals hainite-(Y), rinkite-(Ce) and rinkite-(Y).

Chakhmouradian *et al.* (2008) plotted data for some WGM based only on divalent cations occupying the true octahedral sites. This method suffers from the same issues as Keller and Williams (1995) with large overlaps between different species, especially if data for hiortdahlite is included. Melluso *et al.* (2014) suggested other graphical methods to classify WGM and related species, but also concluded that the high degree of overlap between species and endmembers of species does not make these plots suitable for species determination.

The previously proposed methods for classification do not enable a satisfactory determination at species level from only chemical data. At first glance, the plots by Keller and Williams (1995) do seem to create some distinct groups and it may be possible to separate some species based on them. However, the data presented by Keller and Williams (1995) has in a sense already been filtered as they only presented WGM data. Therefore, these plots may help identify some WGM, but only when it is already known that the chemical data is actually from a WGM. Conversely, they fail when the mineral has not been identified, at least, to a group level. On the basis of the available chemical data it is not possible to make a graphic interpretation to identify WGM or distinguish them from related minerals solely based on chemical data. However, the plots may work if additional methods are applied, for example X-ray diffraction (XRD), to determine if the mineral is a member of the wöhlerite group or another chemically related group e.g. the seidozerite supergroup.

As the graphical methods do not enable distinction of WGM form related mineral groups, let alone identification at species level we have used the same chemical data to establish a workflow for treating chemical data. It must be stressed that the flow below requires the sequential removal of data so that the next step in the flow are criteria to be applied on the remaining data after samples have been removed by the previous step (Fig. 5).

1. Remove poor quality data.
2. Remove data with REE+Y > 0.5 apfu, which are REE-bearing rinkite-group minerals.
3. Remove data with sum Ti+Zr+Hf > 2.5 apfu. This removes seidozerite and grenmarite.
4. Remove data with Fe+Mn > 3 apfu, which will be janhaugite.
5. Remove data where Ca > 5.9 apfu. This step removes cuspidine–baghdadite–niocalite.
6. Remove samples with Ca < 2.9 apfu. This step removes låvenite, normandite and burpalite, but also some kochite.
7. Remove data with Nb+Ta > 0.5 apfu, which corresponds to wöhlerite.
8. Remove data with Ti/(Zr+Hf) < 0.2, which will separate hiortdahlite, moxuanxueite and one data point given as rosenbuschite in the literature.

After these steps a total of 122 data points remain corresponding to götzenite, hainite-(Y), kochite and rosenbuschite. In addition, one data point given as hiortdahlite and the Zr–Ti-cuspidine of Sharygin *et al.* (1996a) remains. The method above provides a good separation of WGM from seidozerite-group minerals.

Solid solution in WGM

The literature often refers to the WGM having a flexible structure resulting in large degree of solid solution (e.g. Perchiazzi *et al.*, 2000; Mitchell and Belton, 2004; Chakhmouradian *et al.*, 2008). Regardless of the diverse composition of the WGM, solid solutions are not as extensive as the chemical data may suggest. There seems to be a high degree of solid solution between cuspidine and niocalite, as well as between cuspidine and baghdadite, however, the solid solution between niocalite and baghdadite is limited (Fig. 4f). In baghdadite, the two Zr sites are edge sharing, resulting in a highly distorted site. If niobium completely replaces Zr, two Nb polyhedra would be edge sharing, which is highly unlikely to happen. Furthermore, a complete replacement of Zr by Nb is not possible as the additional two charges cannot be balanced becasue all anions in baghdadite are already oxygen. A full solid solution would be the coupled substitution $2Zr^{4+} +$

https://doi.org/10.1180/mgm.2022.10 Published online by Cambridge University Press

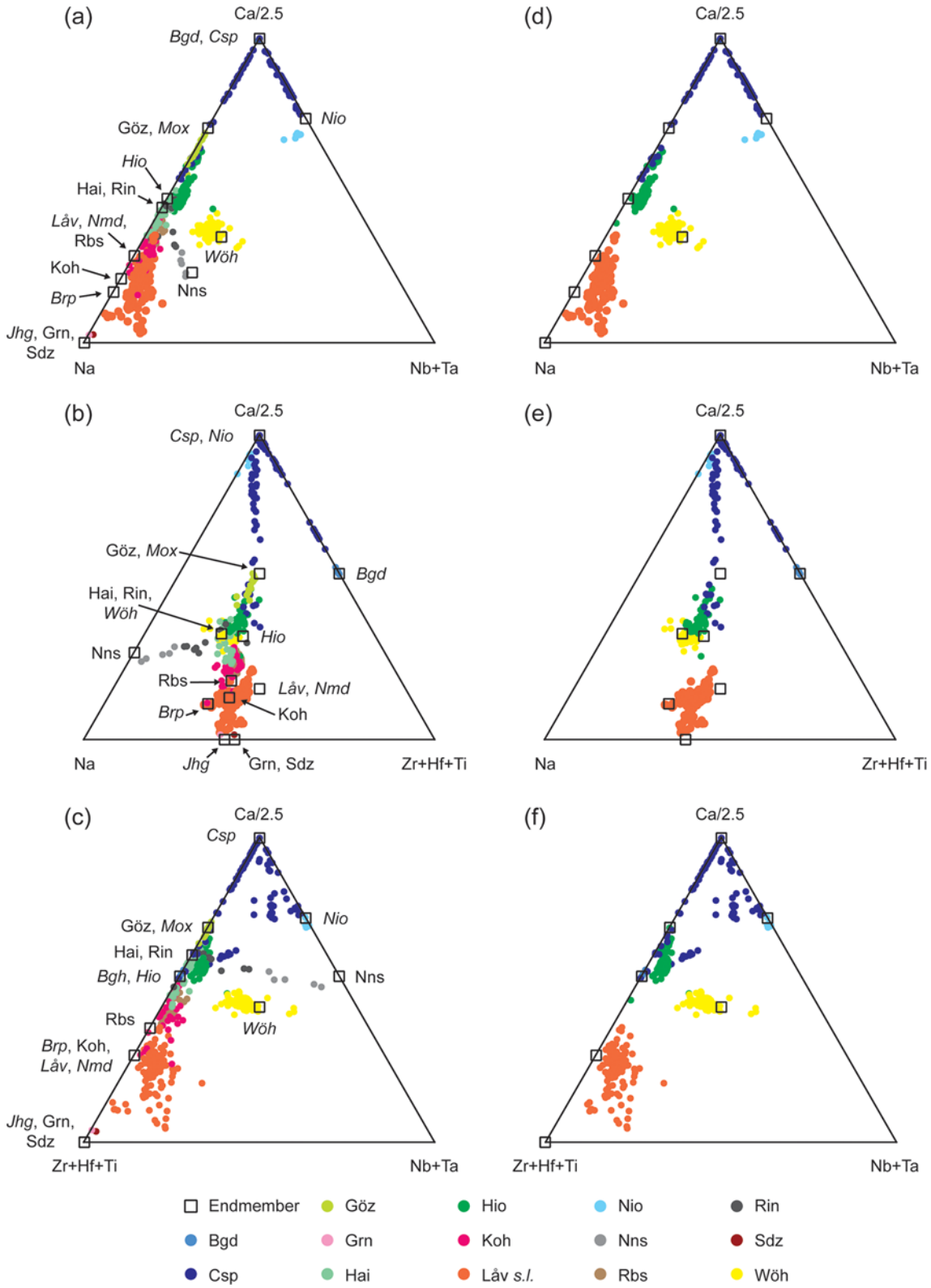

Fig. 4. (a–c) Ternary plots of 650 chemical analyses of WGM and related species from our data and the references listed in the text and (d–f) only WGM. Abbreviations: Baghdadite (Bgd); burpalite (Brp); cuspidine (Csp); götzenite (Göz); grenmarite (Grn); hainite-(Y) (Hai); hiortdahlite (Hio); janhaugite (Jhg); kochite (Koh); låvenite (Låv); moxuanxueite (Mox); niocalite (Nio); normandite (Nmd); nacareniobsite-(Ce) (Nns); rosenbuschite (Rbs); rinkite-(Ce) (Rin); seidozerite (Sdz) and wöhlerite (Wöh). In the figure the abbreviations are in italic for WGM.

https://doi.org/10.1180/mgm.2022.10 Published online by Cambridge University Press

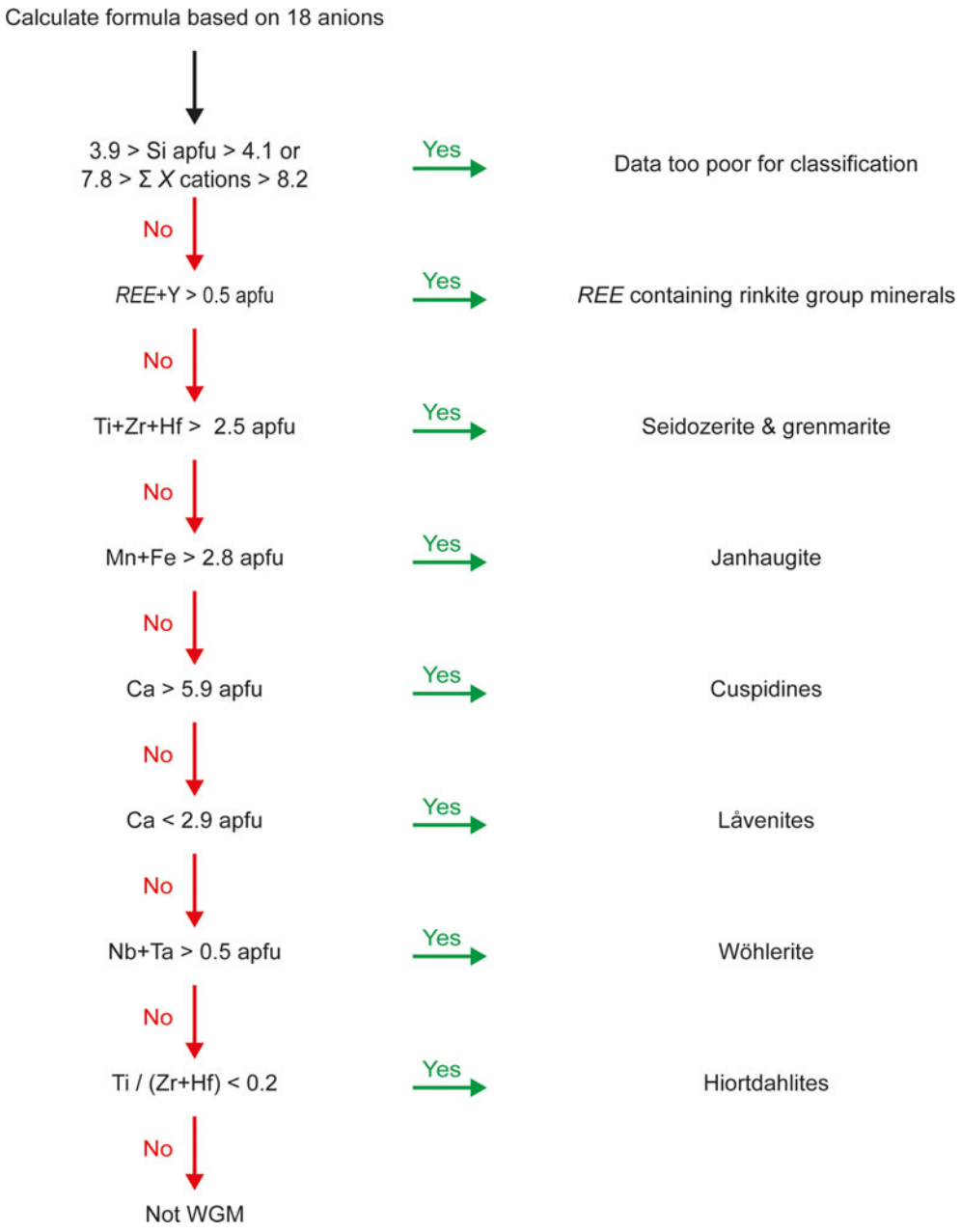

Fig. 5. Schematic workflow for discriminating chemical data into different disilicate groups.

$O^{2-} \leftrightarrow Ca^{2+} + Nb^{5+} + F^{-}$, but this is not a simple substitution as baghdadite and niocalite are not isostructural, and it would lead to a major structural change (Fig. 2). However, it is likely that there is a limited solid solution between the two species as indicated by Casillas *et al.* (2008). Keller and Williams (1995) suggested a degree of solid solution between niocalite and wöhlerite, but most of these data have more than 8.2 apfu *X* site cations and were removed by the above data processing. Wöhlerite and niocalite are not isostructural, therefore solid solution between the minerals not only requires substitution between Ca, Na, Zr and F, but also a change of the position of Nb in the structure between *X*5 and *X*6 (Tables 1,2; Fig. 3).

Sharygin *et al.* (1996a) investigated a series of cuspidine and götzenite minerals from Pian di Celle in Italy and suggested a partial solid solution between cuspidine and an end-member with the composition $NaCa_6Zr(Si_2O_7)_2OF_3$. From powder XRD and Raman spectroscopy Sharygin *et al.* (1996a) showed this phase to be structurally more closely related to hiortdahlite than cuspidine, and in fact this composition corresponds to the recently approved mineral moxuanxueite (Qu *et al.*, 2020).

Extended solid solution has been documented between låvenite and normandite (Perchiazzi *et al.*, 2000) as Zr in låvenite and Ti in normandite both occupy the *X*1 site and hence can replace each other with no additional structural modifications. Similarly, the Mn/Fe ratio differs in låvenite and as both these cations occupy the *X*3 site, it is likely that Fe-equivalent species may be found of both minerals.

In summary, solid solution in the WGM is controlled by the crystal structure and occurs where no major structural modifications are required, e.g. between låvenite and normandite, or

https://doi.org/10.1180/mgm.2022.10 Published online by Cambridge University Press

between cuspidine, baghdadite and niocalite. Therefore, it is not uncommon to find several different WGM in the same rocks as small chemical changes favour the formation of multiple species rather than creating solid-solution series.

Nomenclature for wöhlerite-group minerals

Classification

The general formula for WGM can be expressed as $X_8(Si_2O_7)_2W_4$, without any further distinction among the *X* and *W* sites. As shown in Fig. 2, a specific chemical element will have a different preferential *X* site in different WGM. For instance, high-field-strength elements (HFSE) such as Ti, Zr and Nb, are hosted on crystallographic sites located in different columns of the walls and on different cationic *X* sites. Consequently, there is no crystal-chemical feature to assign elements to specific *X* sites. As a rule, the topological representation of the cationic walls has been made by drawing the projection of the wall along the crystallographic *c* axis. The labelling of the sites always starts with *X*1, which is the smallest site belonging to outer columns of the wall. The site siting in the outer column and connected to *X*1 though edge-sharing is labelled *X*2. Afterwards the sites are labelled in succession, going from the outer to the inner columns of the wall, and according to the symmetry of the mineral. The crystal structure of hiortdahlite is characterised by two cationic walls, where wall I contains the HFSE-dominated site located in the outer column (Fig. 3). The anionic *W* sites correspond to the ligands that are not bonded to the disilicate groups. *W*1 and *W*2 are the anionic sites bonded to *X*1 and *X*2, respectively. Depending of the symmetry of the mineral, *W*3 and *W*4 are either belonging to the same outer column as *W*1 and *W*2, or to the second outer column of the wall. The *W* anionic sites occurring between the two inner columns are the symmetrical equivalents of the *W* sites defined previously.

The classification of WGM is based on the occupancy of the structural *X* and *W* sites, and the different combination of chemical elements on these sites are regarded as different mineral species. Considering only chemical data is in some cases insufficient to correctly identify WGM at a species level. Consequently, a structural refinement is needed for a complete characterisation. The sequential application of the dominant-valency and the dominant-constituent rules is suitable for the determination of the end-member formula (Hatert and Burke, 2008; Bosi *et al.*, 2019b). However, due to the possible occurrence of heterovalent substitutions on both the cationic and anionic sites, in some cases this method may fail to provide an end-member formula fulfilling the end-member definition (Hawthorne, 2021; Hawthorne *et al.*, 2021). Therefore, we suggest using the site-total charge (STC) approach to define the end-member formula (Bosi *et al.*, 2019a, 2019b).

The relative position of the cation or anion inside the structural walls is not a valid criterion to define a new species, as it would lead to a proliferation of the number of species. A mineral phase showing the same chemical composition as previously described species but with a different cationic ordering must be considered as an analogue to that species. Polytypism is likely to occur among WGM (Merlino and Perchiazzi, 1988), and polytypes are not considered as different mineral species (Nickel and Grice, 1998). The polytypes must be described according to the nomenclature proposed in the IMA–CNMNC guidelines (Guinier *et al.*, 1984; Nickel, 1993; Nickel and Grice, 1998).

Name, prefixes and suffixes

All the wöhlerite-group minerals have a distinct name, with no prefix or suffix. Due to the relatively large number of structural sites that are able to host the same cation (e.g. Ca^{2+}), we strongly discourage the use of a compositional suffix (e.g. calcio-, ferro-), as this is unclear to which structural site these prefixes will be related. For the same reason, we also discourage the use of prefix referring to the composition of anionic *W* sites. In the case of a species characterised by one crystallographic site dominated by Y or REE, we recommend using a new rootname as well as the Levinson suffix (Bayliss and Levinson, 1988).

Hiortdahlite end-member formula

In order to define the correct end-member formula of hiortdahlite new chemical data was collected and a crystal structure refinement was performed on a sample from the type locality, Langodden, Langesundsfjord, Norway (samples located in the NHM Oslo collections, catalogue number KNR 24099). The chemical data were acquired using the CAMECA SX100 electron microprobe housed at the Department of Geosciences, University of Oslo. The instrument was operated with a beam current of 15 nA and an acceleration voltage of 15kV, creating a 10 µm spot. The following natural and synthetic standards were used: albite (Na), zircon (Zr), wollastonite (Ca and Si), pyrophanite (Ti and Mn), REE orthophosphate (Y, La, Ce and Nd; Jarosewich and Boatner, 1991), MgO (Mg), Fe metal (Fe), Nb metal (Nb) and fluorite (F). The intensity data were corrected for inter-element overlaps and matrix effects using the PAP routine (Pouchou and Pichoir 1984). The chemical data are compared with those published by Andersen *et al.* (2010) on type-locality material (Table 3).

Single-crystal X-ray data were collected at room temperature with monochromated Mo*K*α radiation (λ = 0.71703 Å – 50 kV and 1 mA) on a Rigaku Synergy-S diffractometer equipped with a HyPix–6000He detector housed at NHM Oslo. The instrument has Kappa geometry and both data collection and

Table 3. Chemical data for hiortdahlite based on the average of 26 point analyses.

	Sample KNR 24099 (This work)				Andersen *et al.* (2010)	
Constituent	Average (wt.%)	S.D. (2σ)	Range	apfu	Average (wt.%)	apfu
Na_2O	6.62	0.30	6.39–6.87	1.66	6.84	1.74
CaO	32.90	0.69	32.32–33.62	4.55	32.77	4.60
Y_2O_3	0.56	0.08	0.48–0.63	0.04	0.48	0.03
La_2O_3	0.09	0.05	0.03–0.16	0.01	0.08	0.01
Ce_2O_3	0.26	0.05	0.21–0.31	0.01	0.30	0.01
Nd_2O_3	0.12	0.14	0.01–0.24	0.01	0.08	0.01
MgO	0.04	0.02	0.02–0.06	0.01	-	-
MnO	0.92	0.12	0.80–1.06	0.10	0.92	0.10
FeO	1.17	0.18	1.00–1.40	0.13	0.87	0.10
TiO_2	0.98	0.12	0.83–1.13	0.10	0.87	0.09
ZrO_2	17.12	0.81	16.32–17.81	1.08	18.21	1.16
HfO_2	-	-	-	-	0.46	0.02
Nb_2O_5	1.90	0.42	1.43–2.28	0.11	1.81	0.11
SiO_2	30.76	0.49	30.23–31.45	3.97	30.52	4.00
F	8.41	0.56	3.33–3.77	3.44	8.21	3.40
O = F	3.54				3.46	
Total	98.31				98.96	

S.D. – standard deviation

https://doi.org/10.1180/mgm.2022.10 Published online by Cambridge University Press

Table 4. Data collection and structure refinement details for hiortdahlite from Langodden, Langesundsfjord, Norway.

Crystal data	
Temperature (K)	293
Space group	$P\bar{1}$
Lattice parameters	
a (Å)	10.9517(1)
b (Å)	10.9251(1)
c (Å)	7.3555(1)
α (°)	109.369(1)
β (°)	109.180(1)
γ (°)	83.873(1)
V (Å^3)	784.17(2)
Z	2
Data collection	
Diffractometer	Rigaku XtaLAB Synergy-S
Detector	Hybrid Photon
Radiation; λ (Å)	Mo$K\alpha$; 0.71073
Absorption coefficient, μ (mm^{-1})	3.293
F(000)	749
θ range (°)	2.79–33.62
Index range	$-17 < h < 17$, $-16 < k < 16$, $-11 < l < 11$
No. of measured reflections	31,302
Total reflections (N_{tot})/unique (N_{ref})	5619/5077
Criterion for observed reflections	$I > 3\sigma(I)$
Refinement	
Refinement on	Full-matrix least-squares on F^2
R, wR ($I > 3\sigma(I)$)	2.52, 2.77
R_2, wR_2 (all reflection)	11.26, 11.73
R_{int} (%)	1.98
No. of refinement parameters (N_{par})	271
Weight scheme	$1/(\sigma^2\|F\|+0.010F^2)$
Max. and min. residual peak (e^- Å^{-3})	−0.68 / 0.56
GoF	1.03

subsequent data reduction, together with face-based absorption corrections were carried out using the Rigaku *CrysAlisPro* software. The details of the data collection and refinement are provided in Table 3. The initial structure solution in space group $P\bar{1}$ was determined by the charge flipping method using the *Superflip* algorithm (Palatinus and Chapuis, 2007), and the structural model was subsequently refined on the basis of F^2 with the *Jana2006* software (Petříček *et al.*, 2014). All atoms were refined with anisotropic thermal parameters. The details of the refinement are provided in Table 4 and the atoms coordinates, anisotropic thermal parameters and detailed bond distances are provided in the Supplementary tables S1, S2 and S3. Free refinement of the site-scattering factors showed that the *X*3 (Na), *X*4 (Ca) and *X*6 (Ca) sites were fully occupied, and that *X*1 (Zr), *X*2 (Ca) and *X*5 (Ca) sites were slightly deviating from a full occupancy. To extract accurate site-scattering factors, mixed occupancies Zr + Ca (*X*7) and Ca + Na (*X*8) were refined. The empirical formula is recalculated on the basis of (O+F) = 18 apfu. The site-scattering factors and the established cationic distribution in the crystal structure are provided in Table 5 and the bond-valence table is provided in Table 6. The crystallographic information file has been deposited with the Principal Editor of *Mineralogical Magazine* and is available as Supplementary material.

As shown by Merlino and Perchiazzi (1985), the main chemical substitutions occur on the *X*7 and *X*8 sites and the bond-valence analysis indicate a mixed $O^{2-} + F^-$ occupancy on the anionic *W*1 site (Table 7). The refinement of the site scattering for the Ca1 (*X*2) and Ca3 (*X*5) sites shows a deficit and an excess of electronic density, respectively. Therefore, considering the average bond distances around these sites, Ca + Na and Ca + Y + REE

Table 5. Site population assignment and structural parameters for the crystal structure of hiortdahlite.

Site	RSS	Site-population (apfu)	CSS	ABL	CBL
*X*1	38.4	$Zr_{0.79}Nb_{0.11}Ti_{0.10}$	38.3	2.084	2.100
*X*2	18.8	$Ca_{0.85}Na_{0.15}$	18.7	2.515	2.549
*X*3	11.0	$Na_{1.00}$	11.0	2.444	2.420
*X*4	20.0	$Ca_{1.00}$	20.0	2.407	2.460
*X*5	21.0	$Ca_{0.93}Y_{0.04}Ce_{0.03}$	21.9	2.340	2.396
*X*6	20.0	$Ca_{1.00}$	20.0	2.378	2.400
*X*7	26.6	$Ca_{0.48}Zr_{0.29}Fe_{0.13}Mn_{0.10}$	27.1	2.231	2.230
*X*8	14.4	$Na_{0.60}Ca_{0.40}$	14.6	2.567	2.576

RSS: Refined site scattering (epfu); CSS: calculated site scattering (epfu); ABL: average observed bond-distances (Å); CBL: calculated averaged bond-distances (Å), using the ionic radii of Shannon (1976).

have also been refined on these sites, respectively (Table 5). All Nb, Ti and Hf has been attributed to the *Zr* site (*X*1), which was then filled up with Zr. The remaining Zr was attributed to the *X*7 sites, along with all the Mn and Fe content. The *X*7 site was then filled with Ca. Refinement of the site scattering in the *X*8 position indicates an excess of electron density and therefore Ca was assumed to replace Na. The cationic distribution proposed is in excellent agreement with the different structural parameters and the bond-valence analysis (Tables 5, 6). Bond-valence sums show that the *W*2, *W*3 and *W*4 sites are populated by F^- and that a substitution $O^{2-} \leftrightarrow F^-$ is occurring on the *W*1 site (Table 6). Taking into account previous work and the new data presented here, the end-member formula of hiortdahlite is $Na_2Ca_4(Ca_{0.5}Zr_{0.5})Zr(Si_2O_7)_2OF_3$, with a constrained mixed occupancy of $Ca_{0.5}Zr_{0.5}$ $(M^{2+}_{0.5}M^{4+}_{0.5})^{\Sigma 3+}$, in order to obtain a charge-balanced formula.

The refinement provided in this work is slightly different than the one proposed by Biagioni *et al.* (2012) on a mineral phase structurally related to hiortdahlite (Table 7). The incorporation of Ti^{4+} on the larger *X*7 site (<*X*7–O> = 2.233Å) instead of the smaller *X*1 site (<*X*1–O> = 2.082Å) is unlikely considering the ideal bond distance for octahedrally coordinated Ti (2.005Å, Shannon (1976); Table 5, S3). The partitioning of Y and REE between the *X*5 and *Na* sites (*X*3) is not clear, however, we have not detected a refined site-scattering factor higher than 11 epfu for the *X*3 site in our investigations.

Hiortdahlite and moxuanxueite are the only approved WGM with a structure containing two topologically independent octahedral walls. The ideal compositions of the walls are given by $^{\text{wall-I}}[^{X1}Zr^{X2}Ca^{X3}Na^{X4}Ca]$ and $^{\text{wall-II}}[^{X5}Ca^{X6}Ca^{X7}(Zr_{0.5}Ca_{0.5})^{X8}Na]$. The chemical compositions of the walls are similar, although in the first wall the *Zr* site is in the outer columns, while in the second wall the *X*7 site is in the central columns. Note that both walls in hiortdahlite are topologically and chemically unique among the WGM (Table 2).

Discreditation of marianoite

Marianoite was discovered from the silicocarbonatite Prairie Lake complex, Ontario, Canada (Chakhmouradian *et al.*, 2008), and was considered the Nb-analogue of wöhlerite. Its simplified formula is $Na_2Ca_4(Nb,Zr)_2(Si_2O_7)_2(O,F)_4$. Marianoite was described as monoclinic, $P2_1$, with $a = 10.846$, $b = 10.226$, $c = 7.273$ Å and $\beta = 109.33°$. The highest Nb content reported by Chakhmouradian *et al.* (2008) for marianoite is 1.019 apfu, which is roughly 0.3 apfu more than in wöhlerite from the Langesundsfjord (Sunde

https://doi.org/10.1180/mgm.2022.10 Published online by Cambridge University Press

Table 6. Detailed bond-valence table (vu) for the crystal structure of hiortdahlite.

	*X*1	*X*2	*X*3	*X*4	*X*5	*X*6	*X*7	*X*8	Si1	Si2	Si3	Si4	Σ
O1	0.46		0.09	0.32					1.02				1.89
O2					0.38	0.26		0.20	1.03				1.88
O3	0.68	0.23						0.06	0.97				1.96
O4		0.18							0.97	0.98			2.13
O5		0.36	0.11	0.39						1.05			1.92
O6					0.33	0.20	0.34			1.01			1.89
O7	0.72	0.19								0.98			1.90
O8				0.09	0.37	0.38					1.09		1.92
O9						0.36	0.41	0.11			1.08		1.95
O10	0.64	0.15		0.29							0.98		2.06
O11		0.16						0.09			0.97	0.95	2.17
O12					0.36	0.39						1.06	1.81
O13	0.62	0.15	0.21									0.96	1.97
O14					0.37		0.45	0.17				1.04	2.02
*W*1	0.72						0.36	0.25					1.71
							0.38						
*W*2		0.29					0.46	0.14					1.08
								0.19					
*W*3			0.17	0.31	0.31								1.07
				0.27									
*W*4			0.15	0.32		0.32							1.00
			0.21										
Σ	3.85	1.71	0.94	2.00	2.12	1.92	2.40	1.21	4.03	4.04	4.11	4.01	
VS	4.11	1.85	1.00	2.00	2.07	2.00	2.58	1.40	4.00	4.00	4.00	4.00	

Bond-valence parameters are recalculated according to the site occupancies and taken from Brown and Altermatt (1985) for the *X*–(O,F) distances and Gagné and Hawthorne (2015) for the Si–O distances. VS: bond-valence sums calculated according to the site occupancy.

Table 7. Site-population assignments in the crystal structure of hiortdahlite and hiortdahlite-related minerals.

		Langesundsfjord [1]	Langodden [2]**	Los Archipelago [3]	Monte Somma [4]
		Hiortdahlite	Hiortdahlite	*	*
a (Å)		11.0149(9)	10.9517(1)	10.991(7)	10.970(2)
b (Å)		10.9409(9)	10.9251(1)	10.934(3)	10.943(1)
c (Å)		7.3534(3)	7.3555(1)	7.366(2)	7.365(3)
α (°)		109.350(3)	109.369(1)	109.60(3)	109.63(2)
β (°)		109.879(4)	109.180(1)	109.43(2)	109.65(2)
γ (°)		83.434(4)	83.873(1)	83.55(3)	83.39(1)
Site					
Ca1	*X*2	$Ca_{1.00}$	$Ca_{0.85}Na_{0.15}$	$Ca_{1.00}$	$Ca_{0.72}Na_{0.28}$
Ca2	*X*6	$Ca_{1.00}$	$Ca_{1.00}$	$Ca_{1.00}$	$Ca_{1.00}$
Ca3	*X*5	$Ca_{1.00}$	$Ca_{0.93}Y_{0.04}REE_{0.03}$	$Ca_{1.00}$	$Ca_{1.00}$
Ca4	*X*4	$Ca_{1.00}$	$Ca_{1.00}$	$Ca_{1.00}$	$Ca_{1.00}$
Zr	*X*1	$Zr_{1.00}$	$Zr_{0.79}Nb_{0.11}Ti_{0.10}$	$Zr_{0.90}Nb_{0.05}Ti_{0.05}$	$Zr_{1.00}$
M	*X*7	$Zr_{0.33}Ti_{0.16}Ca_{0.16}Mn_{0.16}Fe_{0.16}$	$Ca_{0.48}Zr_{0.29}Fe_{0.13}Mn_{0.10}$	$Ca_{0.44}Mn_{0.29}Fe_{0.15}Ti_{0.07}Mg_{0.05}$	$Mn_{0.41}Ca_{0.40}Zr_{0.19}$
Na	*X*3	$Na_{1.00}$	$Na_{1.00}$	$Na_{0.95}REE_{0.05}$	$Na_{1.00}$
NaCa	*X*8	$Na_{0.60}Ca_{0.40}$	$Na_{0.60}Ca_{0.40}$	$Ca_{0.65}Na_{0.35}$	$Na_{0.60}Ca_{0.40}$

*Not hiortdahlite s.s. **Langodden (TL) – Structural formula: $Na_{1.75}Ca_{4.66}Fe_{0.13}Mn_{0.10}Y_{0.04}Ce_{0.03}Zr_{1.08}Nb_{0.11}Ti_{0.10}(Si_2O_7)_2(O_{0.6}F_{0.4})F_3$,
Chemical formula: $Na_{1.66}Ca_{4.55}Fe_{0.13}Mn_{0.10}Y_{0.04}Ce_{0.03}Zr_{1.08}Nb_{0.11}Ti_{0.10}(Si_{1.98}O_7)_2(O_{0.57}F_{0.43})F_3$ (Table 3)
[1] Merlino and Perchiazzi (1985); [2] this work; [3] Biagioni *et al.* (2012); [4] Domain IV, Bellezza *et al.* (2012).

et al, 2018). The approval of marianoite as a valid mineral species was based on the assumption that both Zr and Nb are disordered on the two smallest octahedral sites [average bond lengths: 2.031 (*X*6) and 2.080 Å (*X*1)] occurring in the structure. As a result of the similar X-ray and neutron scattering characteristics of Zr and Nb, it is not possible to solve the ordering issue between these two chemical elements by using standard diffraction methods. Following the description of marianoite, Merlino and Mellini (2009) published a discussion arguing that in wöhlerite and marianoite there is an ordering of Zr and Nb, with Nb preferentially occupying the smallest site (*X*6) and Zr the second smallest octahedra (*X*1) of the structure. The same authors have proposed to solve this question through anomalous scattering using synchrotron radiation sources that will allow Zr and Nb to be distinguished. Bellezza *et al.* (2012) and Biagioni *et al.* (2012) have used an ordered approach in their refinements. Readers are referred to Merlino and Mellini (2009) and Chakhmouradian and Mitchell (2009) for more information on that discussion.

Following the classification system proposed herein for WGM, wöhlerite and marianoite are equivalent. If one considers a complete cationic ordering between Zr^{4+} and Nb^{5+}, the resulting end-member formula for both wöhlerite and marianoite is $Na_2Ca_4{}^{X1}(Zr)^{X6}(Nb)(Si_2O_7)_2O_3F$. The maximum Nb content reported for marianoite is 1.02 apfu (associated with 0.85 Zr pfu) (Chakhmouradian *et al.*, 2008), which is not enough to achieve Nb > Zr on both *X*1 and *X*6 sites and then define a

https://doi.org/10.1180/mgm.2022.10 Published online by Cambridge University Press

Nb-dominant end-member. In the second case, if one considers that Zr^{4+} and Nb^{5+} are disordered, the $X1 + X6$ sites would have a total charge of +9, to keep the charge balance of the formula $Na_2Ca_4(X1)(X6)(Si_2O_7)_2O_3F$. The possible charge arrangements of the dominant cations R occupying the $X1$ and $X6$ sites are (i) $^{X1}(R^{4+}) + {}^{X6}(R^{5+})$ and (ii) $^{X1}(R^{4.5+}) + {}^{X6}(R^{4.5+})$. The charge arrangement (ii) is not valid, because it implies a double occupancy ($Zr^{4+}_{0.5}Nb^{5+}_{0.5}$) on two sites. The charge arrangement (i) leads to the end-member formula $Na_2Ca_4{}^{X1}(R^{4+})^{X6}(R^{5+})(Si_2O_7)_2O_3F$, and to the atomic arrangement $Na_2Ca_4{}^{X1}(Zr^{4+})^{X6}(Nb^{5+})(Si_2O_7)_2O_3F$. The atomic arrangement and the end-member formula are identical to those of wöhlerite. Consequently, marianoite must be considered equivalent to wöhlerite and is discredited.

Comment on the phase 'hiortdahlite II'

'Hiortdahlite II' is not an approved mineral species, although Merlino and Perchiazzi (1987) stated that the name 'hiortdahlite II' was approved by the IMA Commission on New Minerals and Mineral Names (merged with CNMNC in 2006), a subsequent new mineral proposal was never submitted. Hiortdahlite II was described by Aarden and Gittins (1974) in samples from the Kipawa River, Kipawa alkaline complex, Quebec, Canada. Roda Robles *et al.* (2001) reported hiortdahlite II from the Ilímaussaq alkaline complex, Greenland, Tamazeght complex, Morocco, and Iles de Los, Guinea, based on chemical analyses and powder X-ray diffraction. We have analysed material from the same locality in the Ilímaussaq complex, and all of the supposed hiortdahlite II crystals have a unit-cell setting and a crystal structure identical to those of hiortdahlite. Therefore, it may be questionable that hiortdahlite II exists at these localities. This further emphasises the need for full crystal structure refinement to correctly identify WGM at a species level.

Chemical analysis on the 'type' material gave the formula $(Na_{1.70}Ca_{4.02}Mn_{0.04}Fe_{0.02}Mg_{0.02}Al_{0.02}Y_{0.24}REE_{0.08}Zr_{1.16}Nb_{0.04}Ti_{0.02})_{\Sigma 7.36}(Si_{2.05}O_7)_2O_{0.82}OH_{0.36}F_{2.68}$, and therefore hiortdahlite II was interpreted as a cationic-deficient analogue of hiortdahlite (Aarden and Gittins, 1974). However, recent chemical analyses performed on the type material of hiortdahlite (Andersen *et al.*, 2010) indicate roughly the same amount of Zr per unit formula than in the material described by Aarden and Gittins (1974). Note that hiortdahlite II contains up 0.24 Y apfu, while in hiortdahlite from Langodden, the Y content is below 0.05 apfu. The total REE content is also slightly larger in hiortdahlite II than in hiortdahlite.

Hiortdahlite II is reported as triclinic, $P\bar{1}$, with $a = 10.95$, $b = 10.31$, $c = 7.29$ Å, $\alpha = 90.19$, $\beta = 109.02$ and $\gamma = 90.05°$ (Aarden and Gittins, 1974). The crystal structure refinement was performed on samples from Kipawa, and gave a structural model based on two independent topological octahedral walls (Merlino and Perchiazzi, 1987). The wall-I in hiortdahlite II has the same chemical composition as the wall-I in hiortdahlite, though the cationic distribution is not strictly equivalent (Fig. 3). The main difference between species is observed in the topology of wall-II, with a composition of $[^{X5}Ca^{X6}Ca^{X7}(Zr_{0.5}Ca_{0.5})^{X8}Na]$ and $[^{X5}Y^{X6}Ca^{X7}Ca^{X8}(Ca_{0.5}Na_{0.5})]$ in hiortdahlite and hiortdahlite II, respectively. However, the difference between the crystal chemical formula provided by Merlino and Perchiazzi (1987) and the chemical data reported by Aarden and Gittins (1974) is significant, for instance 1.76 Y apfu is reported in the structure while the chemical data indicate 0.32 Y + REE apfu.

Consequently, the presence of a Y-dominant site in the structure of hiortdahlite II is questionable, and new investigations must be performed on hiortdahlite II material to explore if it is a polytype of hiortdahlite or a distinct and valid mineral species. A new mineral proposal would still be required to be submitted to the IMA–CNMNC.

Conclusions

The general formula of the wöhlerite-group minerals is given by $X_8(Si_2O_7)_2W_4$, where X denotes the cations occurring in the polyhedra building the four-column wall, and where W denotes the anionic sites that are not bonded to the disilicate groups. The crystal structure of WGM is characterised by 'octahedral walls' made of four columns of edge-sharing X sites. The symmetry of the different species can vary from monoclinic to triclinic, according to the cationic ordering on the X sites and the relative position of the disilicate groups. Distinction between the mineral species is made based on the dominant elements at the X and W sites, and different combinations of X and W constituents should be regarded as separate mineral species.

In addition to the classification scheme, the following changes have been approved by the IMA–CNMNC: (i) the end-member formula of hiortdahlite has changed to $Na_2Ca_4(Ca_{0.5}Zr_{0.5})Zr(Si_2O_7)_2OF_3$, with a valency-imposed double-site occupancy of $(Ca^{2+}_{0.5}Zr^{4+}_{0.5})^{\Sigma 3+}$ on the $X7$ site, and (ii) marianoite is discredited, as it is structurally and chemically equivalent to wöhlerite.

The chemical variation in WGM results in the formation of individual species rather than solid-solution series. The reason being that despite similar compositions between many of the members they are not isostructural, therefore, heterovalent substitutions typically require a complete reorder of the structure. Such reorders appear energetically unfavourable compared to the formation of another species, commonly resulting in rocks containing several WGM or even seidozerite supergroup minerals. Furthermore, the co-existence of different WGM and seidozerite-supergroup minerals in the same rock makes it a challenge for petrologists to identify minerals on a species level. We proposed a discrimination flow-chart for separating various WGM from chemically related species.

Acknowledgements. We thank Marco Pasero and all members of the IMA–CNMNC for their helpful suggestions and comments. Muriel Erambert is thanked for her assistance with the EMPA data collection of the hiortdahlite material. We wish to thank Qu Kai for the discussion around moxuanxueite. We are grateful to George Christidis and Patrick Woodward for Editorial handling and we thank Anton Chakhmouradian and three additional anonymous reviewers for their comments on the manuscript.

Supplementary material. To view supplementary material for this article, please visit https://doi.org/10.1180/mgm.2022.10

References

Aarden H.M. and Gittins J. (1974) Hiortdahlite from Kipawa river, Villedieu township, Temiscaming County, Québec, Canada. *The Canadian Mineralogist*, **12**, 241–247.

Andersen T., Erambert M., Larsen A.O. and Selbekk R.S. (2010) Petrology of nepheline syenite pegmatites in the Oslo rift, Norway: Zirconium silicate mineral assemblages as indicators of alkalinity and volatile fugacity in mildly agpaitic magma. *Journal of Petrology*, **51**, 2303–2325.

Andreeva I.A., Kovalenko V.I., Nikiforov A.V. and Kononkova N.N. (2007) Compositions of magmas, formation conditions, and genesis of carbonate-bearing ijolites and carbonatites of the Belaya Zima alkaline carbonatite complex, eastern Sayan. *Petrology*, **15**, 551–574.

Annehed H., Falth L. and Raade G. (1985) The crystal structure of janhaugite, a sorosilicate of the cuspidine family. *Neues Jahrbuch fur Mineralogie, Monatshefte*, **1985**, 7–18.

Appel P.W.U., Bigi S. and Brigatti M.F. (1999) Crystal structure and chemistry of yuanfuliite and its relationships with warwickite. *European Journal of Mineralogy*, **11**, 483–491.

Atencio D., Coutinho J.M.V., Ulbrich M.N.C., Vlach S.R.F., Rastsvetaeva R.K. and Pushcharovsky D.Yu. (1999) Hainite from Poços de Caldas, Minas Gerais, Brazil. *The Canadian Mineralogist*, **37**, 91–98.

Bayliss P. and Levinson A.A. (1988) A system of nomenclature for rare-earth mineral species: Revision and extension. *American Mineralogist*, **73**, 422–423.

Bellezza M., Merlino S. and Perchiazzi N. (2004a) Chemical and structural study of the Zr,Ti-disilicates in the venanzite from Pian di Celle, Umbria, Italy. *European Journal of Mineralogy*, **16**, 957–969.

Bellezza M., Franzini M., Larsen A.O., Merlino S. and Perchiazzi N. (2004b) Grenmarite, a new member of the götzenite-seidozerite-rosenbuschite group from the Langesundsfjord district, Norway: definition and crystal structure. *European Journal of Mineralogy*, **16**, 971–978.

Bellezza M., Merlino S. and Perchiazzi N. (2012) Distinct domains in "guarinite" from Monte Somma, Italy: Crystal structures and crystal chemistry. *The Canadian Mineralogist*, **50**, 531–548.

Biagioni C., Bonaccorsi E., Perchiazzi N. and Merlino S. (2010) Single crystal refinement of the structure of baghdadite from Fuka (Okayama Prefecture, Japan). *Periodico di Mineralogia*, **79**, 1–9.

Biagioni C., Merlino S., Parodi G.C. and Perchiazzi N. (2012) Crystal chemistry of minerals of the wöhlerite group from the Los Archipelago, Guinea. *The Canadian Mineralogist*, **50**, 593–609.

Bigi S., Brigatti M.F. and Capedri S. (1991) Crystal chemistry of Fe- and Cr-rich warwickite. *American Mineralogist*, **76**, 1380–1388.

Bosi F., Biagioni C. and Oberti R. (2019a) On the chemical identification and classification of minerals. *Minerals*, **9**, 591–602.

Bosi F., Hatert F., Hålenius U., Pasero M., Miyawaki R. and Mills S.J. (2019b) On the application of the IMA-CNMNC dominant-valency rule to complex mineral compositions. *Mineralogical Magazine*, **83**, 627–632.

Brøgger W.C. (1884) Forelöbig meddelelse om to nye norske mineraler, låvenit og cappelenit. *Geologiska Föreningens i Stockholm Förhandlingar*, **7**, 598–600.

Brøgger W.C. (1890a) Die Mineralien der Syenitpegmatitgänge der Südnorwegischen Augit- und Nephelinsyenite. *Zeitschrift für Krystallographie und Mineralogie*, **16**, 1–690.

Brøgger W.C. (1890b) Vorläufige mittheilung über den „Hiortdahlit", ein neues mineral von Arö, Norwegen. *Nyt Magazin for Naturvidenskabena*, **31**, 232–239.

Brown I.D. and Altermatt D. (1985) Bond-valence parameters obtained from a systematic analysis of the Inorganic Crystal Structure Database. *Acta Crystallographica*, **B41**, 244–247, with updated parameters from https://www.iucr.org/resources/data/datasets/bond-valence-parameters.

Casillas R., Nagy G., Demény A., Ahijado A. and Fernández C. (2008) Cuspidine-niocalite-baghdadite solid solutions in the metacarbonatites of the Basal Complex of Fuerteventura (Canary Islands). *Lithos*, **105**, 25–41.

Chakhmouradian A.R., Mitchell R.H., Burns P.C., Mikhailova Y. and Reguir E.P. (2008) Marianoite, a new member of the cuspidine group from the Prairie Lake silicocarbonatite, Ontario. *The Canadian Mineralogist*, **46**, 1023–1032.

Chakhmouradian A.R. and Mitchell R.H. (2009) Marianoite, a new member of the cuspidine group from the Prairie Lake silicocarbonatite, Ontario: Reply. *The Canadian Mineralogist*, **47**, 1280–1282.

Chakrabarty A., Mitchell R.H., Ren M., Sen A.K. and Pruseth K.L. (2013) Rinkite, cerianite-(Ce), and hingganite-(Ce) in syenite gneisses from the Sushina Hill Complex, India: occurrence, compositional data and petrogenetic significance. *Mineralogical Magazine*, **77**, 3137–3153.

Chakrabarty A., Mitchell R.H., Ren M., Pal S., Pal S. and Sen A.K. (2018) Nb-Zr-REE Re-mobilization and implications for transitional agpaitic rock formation: insights from the Sushina Hill complex, India. *Journal of Petrology*, **59**, 1899–1938.

Chao G.Y. and Gault R.A. (1997) Normandite, the Ti-analogue of låvenite from Mont Saint-Hilaire, Quebec. *The Canadian Mineralogist*, **35**, 1035–1039.

Chen W., Simonetti A. and Burns P.C. (2013) A combined geochemical and geochronological investigation of niocalite from the Oka Carbonatite Complex, Canada. *The Canadian Mineralogist*, **51**, 785–800.

Christiansen C.C., Johnsen O. and Makovicky E. (2003) Crystal chemistry of the rosenbuschite group. *The Canadian Mineralogist*, **41**, 1203–1224.

Comin-Chiaramonti P., Renzulli A., Ridolfi F., Enrich G.E.R., Gomes C.B., De Min A., Azzone R.G. and Ruberti E. (2016) Late-stage magmatic to deuteric/metasomatic accessory minerals from the Cerro Boggiani agpaitic complex (Alto Paraguay Alkaline Province). *Journal of South American Earth Sciences*, **71**, 248–261.

Eggleton R.A., Halford G.E. and Beams S.D. (1979) Hiortdahlite from Jingera, New South Wales. *Journal of the Geological Society of Australia*, **26**, 81–85.

Federico M. and Peccerillo A. (2002) Mineral chemistry and petrogenesis of granular ejecta from the Alban Hills volcano. *Mineralogy and Petrology*, **74**, 223–252.

Ferguson A.K. (1978) The occurrence of ramseyite, titan-låvenite and a fluorine-rich eucolite in a nepheline-syenite inclusion from Tenerife, Canary Islands. *Contribution to Mineralogy and Petrology*, **66**, 15–20.

Friis H., Balić Žunić T., Williams T. and Petersen O.V. (2010) Minerals of the låvenite group from South Greenland and Norway. *Norsk Bergverksmuseet Skrift*, **43**, 35–39.

Gagné O.C. and Hawthorne F.C. (2015) Comprehensive derivation of bond-valence parameters for ion pairs involving oxygen. *Acta Crystallographica*, **B71**, 562–578.

Galuskin E.V., Pertsev N.N., Armbruster T., Kadiyski M., Zadov A.E., Galuskina I.O., Dzierzanowski P., Wrzalik R. and Kislov E.V. (2007) Dovyrenite Ca6Zr[Si2O7]2(OH)4 - a new mineral from skarned carbonate xenoliths in basic-ultrabasic rocks of the Ioko-Dovyren Massif, Northern Baikal Region, Russia. *Mineralogia Polonica*, **38**, 15–28.

Gałuskina I.O., Gałuskin E.V., Lazic B., Armbruster T., Dzierżanowski P., Prusik K. and Wrzalik R. (2010) Eringaite, $Ca_3Sc_2(SiO_4)_3$, a new mineral of the garnet group. *Mineralogical Magazine*, **74**, 365–373.

Golyshev M., Otroshchenko L.P., Simonov V.I. and Belov N.V. (1973) Refining the atomic structure of wöhlerite, $NaCa_2(Zr,Nb)[Si_2O_7](F,O)_2$. *Soviet Physics – Doklady*, **18**, 287–289.

Guarino V., De' Gennaro R., Melluso L., Ruberti E. and Azzone R.G. (2019) The Transition from miaskitic to agpaitic rocks, as highlighted by the accessory phase assemblages in the Passa Quatro alkaline complex (southeastern Brazil). *The Canadian Mineralogist*, **57**, 339–361.

Guinier A., Bokij G.B., Boll-Dornberger K., Cowley J.M., Dŭrovič S., Jagodzinski H., Krishna P., de Wolff P.M., Zvyagin B.B., Cox D.E., Goodman P., Hahn Th., Kuchitsu K. and Abrahams S.C. (1984) Nomenclature of polytype structures. Report of the International Union of Crystallography Ad-Hoc Committee on the nomenclature of disordered, modulated and polytype structures. *Acta Crystallographica*, **A40**, 399–404.

Hatert F. and Burke E.A.J (2008) The IMA–CNMNC dominant-constituent rule revisited and extended. *The Canadian Mineralogist*, **46**, 717–728.

Hawthorne F. (2021) Proof that a dominant endmember formula can always be written for a mineral or a crystal structure. *The Canadian Mineralogist*, **59**, 159–167.

Hawthorne F.C., Mills S.J., Hatert F. and Rumsey M.S. (2021) Ontology, archetypes and the definition of "mineral species". *Mineralogical Magazine*, **85**, 125–131.

Hermezi H.M., McKie D. and Hall A.J. (1986) Baghdadite, a new calcium zirconium silicate mineral from Iraq. *Mineralogical Magazine*, **50**, 119–123.

Jamtveit B., Dahlgren S. and Austrheim H. (1997) High-grade contact metamorphism of calcareous rocks from the Oslo Rift, Southern Norway. *American Mineralogist*, **82**, 1241–1254.

Jarosewich E. and Boatner L.A. (1991) Rare-earth element reference samples for electron microprobe analysis. *Geostandards Newsletter*, **15**, 397–399.

Jones A.P. and Larsen L.M. (1985) Geochemistry and REE minerals of nepheline syenites from the Motzfeldt Centre, South Greenland. *American Mineralogist*, **70**, 1087–1100.

Kapustin Y.L. and Bykova A.V. (1965) First find of hiortdahlite in the USSR. *Doklady Akad. Nauk SSSR*, **161**, 121–124.

Keller J. and Williams C.T. (1995) Niocalite and wöhlerite from the alkaline and carbonatite rocks at Kaiserstuhl, Germany. *Mineralogical Magazine*, **59**, 561–566.

https://doi.org/10.1180/mgm.2022.10 Published online by Cambridge University Press

Khadem Allah B. (1993) *Syénites et pegmatites néphéliniques du complexe alcalin du Tamazeght (Haut Atlas de Midelt, Maroc)*. Thèse de doctorat, Université Paul-Sabatier, Toulouse, France.

Krzątała A., Galuskin E.V., Galuskina I.O. and Vapnik Y. (2018) "Uranian cuspidine" – a potentially new mineral from paralava of Eastern Gurim, Hatrurim Complex, Israel. *Abstracts of the 22nd IMA Meeting*, Melbourne, Australia, 358.

Larsen A.O. (2010) *The Langesundsfjord: History, Geology, Pegmatites, Minerals*. Bode, Verlag BmbH, Salzhemmerdorf, Germany, 239 pp.

Li T.J., Simonov V.I. and Belov N.V. (1966) The crystal structure of niokalite. *Soviet Physics – Doklady*, **11**, 197–199.

Mariano A.N. and Roeder P.L. (1989) Wöhlerite: Chemical composition, cathodoluminescence and environment of crystallization. *The Canadian Mineralogist*, **27**, 709–720.

Matsubara S. and Miyawaki R. (1999) Baghdadite from the Akagana Mine, Iwate Prefecture, Japan. *Bulletin of the National Museum of Nature and Science, Series C*, **25**, 65–72.

Mellini M. (1981) Refinement of the crystal structure of låvenite. *Tschermaks Mineralogische und Petrographische Mitteilungen*, **28**, 99–112.

Mellini M. (1982) Niocalite revised: twinning and crystal structure. *Tschermaks Mineralogische und Petrographische Mitteilungen*, **30**, 249–266.

Mellini M. and Merlino S. (1979) Refinement of the crystal structure of wöhlerite. *Tschermaks Mineralogische und Petrographische Mitteilungen*, **26**, 109–123.

Melluso L., Morra V., Guarino V., De' Gennaro R., Franciosi L. and Grifa C. (2014) The crystallization of shoshonitic to peralkaline trachyphonolitic magmas in a H_2O-Cl-F-rich environment at Ischia (Italy), with implications for the feeder system of the Campania Plain volcanos. *Lithos*, **210–211**, 242–259.

Melluso L., Guarino V., Lustrino M., Morra V. and De' Gennaro R. (2017) The REE- and HFSE-bearing phases in the Itatiaia Alkaline Complex (Brazil), and geochemical evolution of feldspar-rich felsic melts. *Mineralogical Magazine*, **81**, 217–250.

Merlino S. and Mellini M. (2009) Marianoite, a new member of the cuspidine group from the Prairie Lake silicocarbonatite, Ontario: Discussion. *The Canadian Mineralogist*, **47**, 1275–1279.

Merlino S. and Perchiazzi N. (1985) The crystal structure of hiortdahlite I. *Tschermaks Mineralogische und Petrographische Mitteilungen*, **34**, 297–310.

Merlino S. and Perchiazzi N. (1987) The crystal structure of hiortdahlite II. *Mineralogy and Petrology*, **37**, 25–35.

Merlino S. and Perchiazzi N. (1988) Modular mineralogy of the cuspidine group of minerals. *The Canadian Mineralogist*, **26**, 933–943.

Merlino S., Perchiazzi N., Khomyakov A.P., Pushcharovsky D.Y., Kulikova I.M. and Kuzmin V.I. (1990) Burpalite, a new mineral from Burpalinskii massif, North Transbajkal, USSR: its crystal structure and OD character. *European Journal of Mineralogy*, **2**, 177–185.

Mills S.J., Hatert F., Nickel E.H. and Ferraris G. (2009) The standardisation of mineral group hierarchies: application to recent nomenclature proposals. *European Journal of Mineralogy*, **21**, 1073–1080.

Mitchell R.H. and Belton F. (2004) Niocalite-cuspidine solid solution and manganoan monticellite from natrocarbonatite, Oldoinyo Lengai, Tanzania. *Mineralogical Magazine*, **68**, 787–799.

Miyawaki R., Hatert F., Pasero M. and Mills S.J. (2020) IMA Commission on New Minerals, Nomenclature and Classification (CNMNC) Newsletter 57. *Mineralogical Magazine*, **84**, 791–794.

Nickel E.H. (1956) Niocalite – a new calcium niobium silicate mineral. *American Mineralogist*, **41**, 785–786.

Nickel E.H. (1993) Standardisation of polytype suffixes. *Mineralogical Magazine*, **57**, 757–757.

Nickel E.H. and Grice J.D. (1998) The IMA Commission on New Minerals and Mineral Names: procedures and guidelines on mineral nomenclature. *The Canadian Mineralogist*, **36**, 913–926.

Nickel E.H., Rowland J.F. and Mawwell J.A. (1958) The composition and crystallography of niocalite. *The Canadian Mineralogist*, **6**, 264–272.

Owens B.E. and Kremser P.T. (2010) Åkermanite breakdown to cuspidine-bearing sympectite in a calc-silicate xenolith, Kiglapait intrusion, Labrador, Canada. *The Canadian Mineralogist*, **48**, 809–819.

Palatinus L. and Chapuis G. (2007) Superflip – a computer program for the solution of crystal structures by charge flipping in arbitrary dimensions. *Journal of Applied Crystallography*, **40**, 786–790.

Pauling L. (1929) The principles determining the structure of complex ionic crystals. *Journal of the American Chemical Society*, **51**, 1010–1026.

Pautov L.A., Agakhanov A.A., Karpenko V.Yu., Uvarova Yu.A., Sokolova E. and Hawthorne F.C. (2019) Rinkite-(Y), $Na_2Ca_4YTi(Si_2O_7)_2OF_3$, a seidozerite-supergroup TS-block mineral from the Darai-Pioz alkaline massif, the Tien-Shan mountains, Tajikistan: Description and crystal structure. *Mineralogical Magazine*, **83**, 373–380.

Perchiazzi N., McDonald A.M., Gault R.A., Johnsen O. and Merlino S. (2000) The crystal structure of normandite and its crystal-chemical relationships with låvenite. *The Canadian Mineralogist*, **38**, 641–648.

Petříček V., Dušek M. and Palatinus L. (2014) Crystallographic computing system Jana2006: General features. *Zeitschrift Für Kristallographie*, **229**, 345–352.

Portnov A.M., Simonov V.I. and Sinyugina G.P. (1966) Rombic lävenite, a new variety of lävenite. *Doklady Akademii Nauk SSSR*, **166**, 1199–1202.

Portnov A.M. and Sidorenko G.A. (1975) New data on orthorhombic låvenite. *Trudy Mineral Muzeya Akademiya Nauk SSSR*, **24**, 203–206.

Pouchou J.L. and Pichoir F. (1984) A new model for quantitative X-ray microanalysis. I. Application to the analysis of homogeneous samples. *La Recherche Aérospatiale*, **3**, 13–38.

Qu K., Dong G., Li T., Fan G., Wang Y., Cheng Y., Jin R., Sun X., Zhao F. and Wang Y. (2020) Moxuanxueite, IMA 2019-100. CNMNC Newsletter No. 58. *Mineralogical Magazine*, **84**, https://doi.org/10.1180/mgm.2020.93

Raade G. and Mladeck M.H. (1983) Janhaugite, $Na_3Mn_3Ti_2Si_4O_{15}(OH,F,O)_3$, a new mineral from Norway. *American Mineralogist*, **68**, 1216–1219.

Reusser E. (2010) Mineralogical and geochemical characterization of ashes from an early phase of the explosive September 2007 eruption of Oldoinyo Lengai (Tanzania). *Journal of African Earth Sciences*, **58**, 752–763.

Roda-Robles E., Fontan F., Monchoux P., Sørensen H. and de Parseval P. (2001) Hiortdahlite II from the Ilímaussaq alkaline complex, South Greenland, the Tamazeght complex, Morocco, and the Iles de Los, Guinea. *Geology of Greenland Survey Bulletin*, **190**, 131–137.

Rønsbo J.G., Sørensen H., Roda-Robles E., Fontan F. and Monchoux P. (2014) Rinkite-nacareniobsite-(Ce) solid solution series and hainite from the Ilímaussaq alkaline complex: occurrence and compositional variation. *Bulletin of the Geological Society of Denmark*, **62**, 1–15.

Saburi S., Kawahara A., Henmi C., Kusachi I. and Kihara K. (1977) The refinement of the crystal structure of cuspidine. *Mineralogical Journal*, **8**, 286–298.

Scacchi A. (1876) Della cuspidina e del neocrisolito, nuovi minerali vesuviani. *Rendiconto dell'Accademia delle Scienze Fisiche e Matematiche* (*sezione della Societa reale di Napoli*), **15**, 208–209.

Scheerer T. (1843) Ueber den Wöhlerit, eine neue Mineralspecies. *Annalen der Physik und Chemie*, **59**, 327–336.

Shannon R.D. (1976) Revised effective ionic radii and systematic studies of interatomic distances in halides and chalcogenides. *Acta Crystallographica*, **A32**, 751–767.

Sharygin V.V., Stoppa F. and Kolesov B.A. (1996a) Zr-Ti disilicates from the Pian di Celle volcano, Umbria, Italy. *European Journal of Mineralogy*, **8**, 1199–1212.

Sharygin V.V., Stoppa F. and Kolesov B.A. (1996b) Cuspidine in melilitolites of San Venanzo, Italy. *Doklady Akademii Nauk*, **348**, 800–804

Shibayeva R.I. and Belov. N.V. (1962) Crystal structure of wöhlerite, $Ca_2Na(Zr,Nb)Si_2O_7(O,F)_2$. *Doklady Akademii Nauk SSSR*, **146**, 897–900.

Shiraga K., Kusachi I., Kobayashi S. and Yamakawa J. (2001) Baghdadite from Fuka, Okayama prefecture, Japan. *Journal of Mineralogical and Petrological Sciences*, **96**, 43–47.

Simonov V.I. and Belov. N.V. (1960) Crystal structure of låvenite. *Doklady Akademii Nauk SSSR*, **130**, 1333–1336.

Smirnova R.F., Rumanova. I.M. and Belov. N.V. (1955) Crystal structure of cuspidine. *Zapiski Vsesoyuznogo Mineralogicheskogo Obshchestva*, **84**(2), 159–169.

Sokolova E. and Cámara F. (2017) The seidozerite supergroup of TS-block minerals: nomenclature and classification, with change of the following names: rinkite to rinkite-(Ce), mosandrite to mosandrite-(Ce), hainite to

https://doi.org/10.1180/mgm.2022.10 Published online by Cambridge University Press

hainite-(Y) and innelite-1T to innelite-1A. *Mineralogical Magazine*, **81**, 1457–1484.

Stoppa F., Sharygin V.V. and Cundari A. (1997) New mineral data from the kamafugite-carbonatite association: the melilitolite from Pian di Celle, Italy. *Mineralogy and Petrology*, **61**, 27–45.

Sunde Ø., Friis H. and Andersen T. (2018) Variation in major and trace elements of primary wöhlerite as an indicator of the origin of Pegmatites in the Larvik plutonic complex, Norway. *The Canadian Mineralogist*, **56**, 529–542.

Taner M.F., Martin R.F. and Gault R.A. (2013) The mineralogy of Skarns of the spurrite–merwinite subfacies, sanidinite facies, Güneyce–Ikizdere Area, Eastern Black Sea, Turkey. *The Canadian Mineralogist*, **51**, 893–911.

Tilley C.E. (1947) Cuspidine from dolomite contact skarns, Broadford, Skye. *Mineralogical Magazine*, **28**, 90–95.

Vladykin N.V. and Sotnikova I.A. (2017) Petrology, geochemistry and source characteristics of the Burpala alkaline massif, North Baikal. *Geoscience Frontiers*, **8**, 711–719.

Vlasov K.A. (1966) *Geochemistry and Mineralogy of Rare Elements and Genetic Types of Their Deposits. 2. Mineralogy of Rare Elements*. Israel Program Scientific Translations, Jerusalem, Israel.

https://doi.org/10.1180/mgm.2022.10 Published online by Cambridge University Press